



ANNUAL RESEARCH REPORT

2018

Gary S. Was, Director
Ovidiu Toader, Manager and Research Specialist
Fabian Naab, Research Specialist
Ethan Uberseder, Research Specialist
Thomas Kubley, Research Engineer

2600 Draper Road
Department of Nuclear Engineering and Radiological Sciences
University of Michigan
Ann Arbor, Michigan 48109-2145
mibl.engin.umich.edu

Telephone: (734) 936-0131

Fax: (734) 763-4540

The Annual Research Report

This report summarizes the principal research activities in the Michigan Ion Beam Laboratory during the past calendar year. One hundred and thirty researchers conducted 50 projects at MIBL that accounted for 289 irradiations and 9377 hours of instrument usage. The programs included participation from researchers at the University, corporate research laboratories, private companies, government laboratories, and other universities across the United States. These projects also included 7 projects funded through the Nuclear Science User Facility program. The extent of participation of the laboratory in these programs ranged from routine surface analysis to ion assisted film formation. Experiments included Rutherford backscattering spectrometry, elastic recoil spectroscopy, nuclear reaction analysis, direct ion implantation, ion beam mixing, ion beam assisted deposition, and radiation damage by proton bombardment. The following pages contain a synopsis of the research conducted in the Michigan Ion Beam Laboratory during the 2017 calendar year.

About the Laboratory

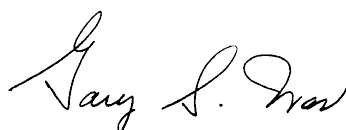
The Michigan Ion Beam Laboratory for Surface Modification and Analysis was completed in October of 1986. The laboratory was established for the purpose of advancing our understanding of ion-solid interactions by providing up-to-date equipment with unique and extensive facilities to support research at the cutting edge of science. Researchers from the University of Michigan as well as industry and other universities are encouraged to participate in this effort.

The lab houses a 3 MV Pelletron accelerator, a 1.7 MV tandem ion accelerator, and a 400 kV ion implanter that are configured to provide for a range of ion irradiation and ion beam analysis capabilities. The control of the parameters and the operation of these systems are mostly done by computers and are interconnected through a local area network, allowing for complete control of irradiations from the control room as well as off-site monitoring and control.

In 2010, MIBL became a Partner Facility of the National Scientific User Facility (NSUF), based at Idaho National Laboratory, providing additional opportunities for researchers across the US to access the capabilities of the laboratory. In 2016, MIBL was recognized as the top ion beam laboratory in the U.S. by the Nuclear Science User Facilities program.

This past year, a 300 kV FEI Tecnai G2 TEM was delivered. Installation was begun along with the fabrication of beamlines 6 and 8 that will interface with the TEM to provide the capability to conduct in-situ irradiation with simultaneous He implantation. Installation of the TEM and beamline connection will be completed in 2018 and the facility will be ready for users by the end of the year.

Respectfully submitted,



Gary S. Was, Director

Research Projects

Nuclear Science User Facility (NSUF) Projects

DEVELOPMENT OF PLANAR DIFFUSION COUPLES WITH REPRESENTATIVE TRISO PYC/SiC MICROSTRUCTURE

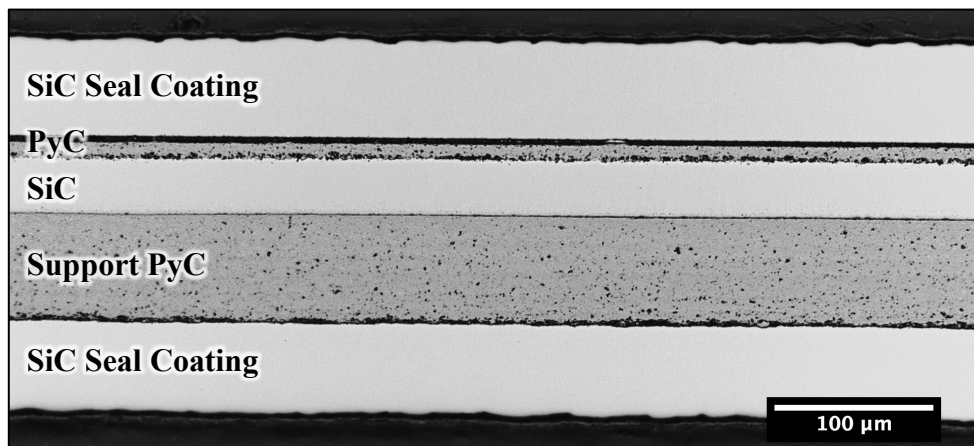
T.J. Gerczak¹, F. Naab², O. Toader²

¹Nuclear Fuel Materials Group, Oak Ridge National Laboratory

²Department of Nuclear Engineering and Radiological Sciences, University of Michigan

Tristructural-isotropic (TRISO) coated particle fuel is the fuel of choice for high temperature gas-cooled reactors. The SiC layer in TRISO fuel is the primary barrier to fission products not retained in the fuel kernel during operation. To ensure safe and efficient operation and improve fuel performance models insight on the release of fission products from intact fuel is required. Planar pyrocarbon (PyC)/silicon carbide (SiC) diffusion couples are being developed with PyC/SiC layers representative of TRISO fuel particles using a fluidized bed chemical vapor deposition (FBCVD) system identical to those used to produce laboratory-scale TRISO fuel for the Advanced Gas Reactor Fuel Qualification and Development Program's first fuel irradiation. The diffusivity of silver, silver and palladium as a system, europium, and strontium in the PyC/SiC system will be studied at elevated temperatures and under high temperature neutron irradiation. The study also includes a comparison of PyC/SiC diffusion couples with varying TRISO layer properties to understand the influence of SiC microstructure (grain size) and the PyC/SiC interface on fission product transport. The first step in accomplishing these goals is the development of the planar diffusion couples. To fabricate the diffusion couples requires multiple steps; fabrication of the primary PyC/SiC structures with targeted layer properties, introduction of fission product species via ion implantation, and seal coating to create an isolated system. The implantations are being carried out at the University of Michigan by the Michigan Ion Beam Laboratory through NSUF access using a 400 kV inline implanter (Blue). Fission product species are implanted into the PyC layer to simulate the pathway for fission products to interact with the SiC layer at the PyC/SiC interface. Initial implantations of the fastest diffusing species, Ag, have been performed to aid in diffusion couple development efforts.

This research is being performed using funding received from the DOE Office of Nuclear Energy's Nuclear Energy University Program through a joint NEET/NEUP R&D with NSUF access award (Project 16-10764).



Example of planar PyC/SiC representative diffusion couple design with SiC seal coating.

IRRADIATION OF THE VANADIUM CARBIDE COATING ON THE T91 STEEL USING PROTONS

K. Jeong, Y. Yang

Nuclear engineering program, department of Materials Science and Engineering, University of Florida

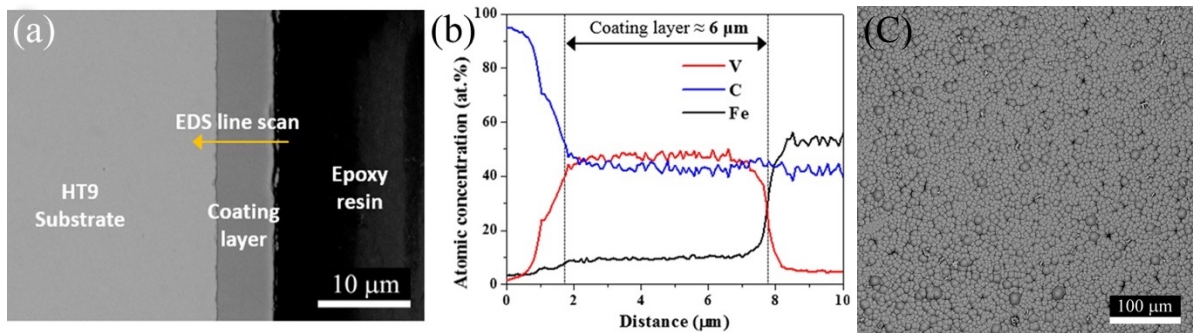
Fuel cladding chemical interaction (FCCI) has long been acknowledged as a problem in the fuel/cladding system and is likely to be exacerbated at high fuel burn-ups and during the use of metallic fuels bearing transuranic elements, as may be the case for sodium-cooled fast reactors (SFR). The fuel cladding inter-diffusion can eventually result in the changes in heat transfer characteristics and the failure of cladding with further breach of fuel into the coolant. One possible solution to mitigating the FCCI is to place a physical barrier between the fuel and cladding. Such a barrier material has to be unsusceptible to interaction at both the fuel and cladding interface. To deposit the vanadium-based coating, a low temperature coating process using organometallic precursor, vanadocene Cp_2V ($Cp=C_5H_5$) was developed, and a vanadium carbide coating was successfully deposited onto a T91 substrate.

As the coating is anticipated to be exposed to high fluence of neutrons along with the cladding in a fast reactor, to ensure the integrity of the coated cladding tube during operation, the irradiation response of the diffusion barrier coating layer and the interfaces in the cladding/coating/fuel systems need to be examined as the coating layer might display a different irradiation response from the substrates. Ion irradiation techniques are especially useful for understanding physical processes of irradiation damage and for screening candidate or new materials for later, in-depth analysis using in-reactor neutron irradiations.

The figure shows the cross-section, plane-view and EDS elemental line scan of the coating layer on the T91 substrate, and the coating was deposited at 400 °C. Figure b shows that the coating contains both V and C. No Fe peak was detected, indicating the surface was well-covered with vanadium carbide coating. The SEM image in left figure shows that approximately 6 μm in thickness coating was obtained and no major gap or de-adhesion between the coating and T91.

The irradiation was conducted on coated flat T91 coupons. To penetrate through the coating layer and to have the interface and substrate irradiated as well, a 2 MeV proton beam was selected. The calculated ion stop range is around 20 μm. The irradiation was conducted at 500 °C that is relevant to a SFR fuel cladding temperature. Three dose conditions of 1, 3, and 5 dpa were performed. The irradiated microstructures of the coating layer and the interfaces is currently investigating using a transmission electron microscope (TEM) with the combination of EDS and electron energy loss spectroscopy (EELS), and will publish a journal paper in the near future.

This work is supported by the U.S. Department of Energy (DOE) Nuclear Energy University Program (NEUP) under award no. DE-NE-0000731.



SEM cross section images, left, EDS line scan profiles, center, and SEM plane view of the specimen coated at 400 °C (right).

STUDY OF THE FACTORS AFFECTING THE RADIATION TOLERANCE OF MAX PHASES FOR INNOVATIVE FUEL CLADDING CONCEPTS

K. Lambrinou¹, B. Tunca^{1,2}, S. Taller³, D. Woodley³, E. Uberseder³, O. Toader³ and G.S. Was³

¹Belgian Nuclear Research Centre, SCK•CEN, Mol, Belgium

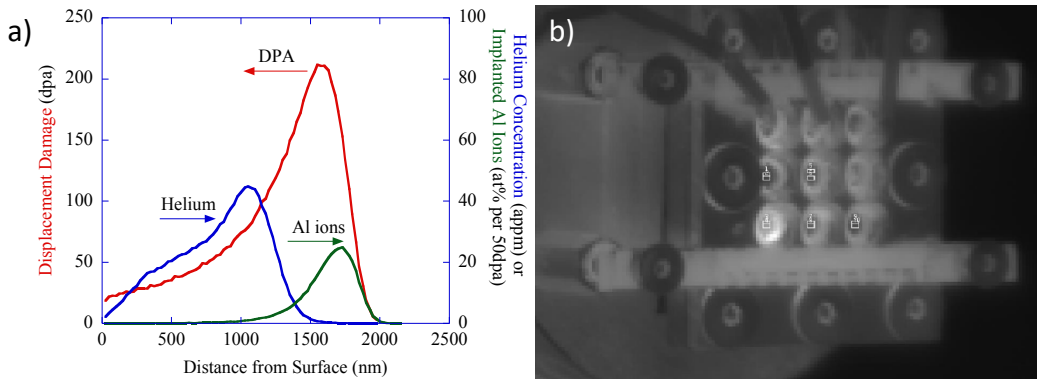
² Department of Materials Engineering, KU Leuven, Heverlee, Belgium

³ Department of Nuclear Engineering & Radiological Sciences, University of Michigan

The goal of this study is to examine the combined effects of composition and texturing on the irradiation tolerance of Nb_4AlC_3 and $(\text{Nb,Zr})_4\text{AlC}_3$ MAX phases. Due their anisotropic crystal structure, MAX phases suffer from anisotropic swelling and micro-cracking as observed in the neutron and ion irradiation studies in literature (Ang et al. 2016; Huang et al. 2015). In this study, for the first time in literature ‘standard grade’ vs. ‘nuclear grade’ MAX phases with improved composition and microstructure were irradiated with $\text{Al}^{++}/\text{He}^{++}$ dual and Al^{++} ion beams. Materials irradiated were produced by Lapauw by synthesizing Nb_4AlC_3 then further improving the properties for potential nuclear applications by alloying with Zr to the optimized composition $(\text{Nb}_{0.85}\text{Zr}_{0.15})_4\text{AlC}_3$ with better fracture toughness (with an improvement from 6.6 ± 0.1 MPa $\text{m}^{1/2}$ to 10.1 ± 0.3 MPa $\text{m}^{1/2}$) and finally texturing to prevent micro-cracking that might occur in randomly textured anisotropic MAX crystals.

To examine the effects of composition and texture on irradiation tolerance, thin (100-200 μm) disks of 3 mm diameter were prepared from Nb_4AlC_3 and $(\text{Nb}_{0.85}\text{Zr}_{0.15})_4\text{AlC}_3$ MAX phases in textured and non-textured condition (in total 4 different grades of material). Four irradiations experiments were performed using Wolverine and Maize accelerators with 4 MeV Al^{++} and 2.18 MeV He^{++} ion beams. Dual beam ($\text{Al}^{++}/\text{He}^{++}$) and single beam (Al^{++}) irradiations were conducted at 330°C and 600°C, temperatures corresponding to the nominal operation temperatures of Gen-III Light Water Reactors (LWR) and Gen-IV Lead Fast Reactors (LFR). The figure (a) below shows the damage profile, in which a total dose of 40 displacements per atom (dpa) at 600 nm depth was collected with a total fluence of 6.26×10^{17} ions/ cm^2 . Temperature control was made with thermocouples, spot-welded on to the reference MAX phase and steel disks that were not irradiated, the sample stage can be seen in figure (b). Thermocouple measurements were used to calibrate the thermal imaging for the temperature determination of MAX phase disks under irradiation. Pressure, temperature and beam currents were recorded during the irradiation experiments.

This work was supported by the U.S. Department of Energy, Office of Nuclear Energy under DOE Idaho Operations Office Contract DE-AC07-051D14517 as part of a Nuclear Science User Facilities experiment.



Displacement and implantation curves for 4 MeV Al^{2+} and energy degraded He^{2+} in MAX phase ceramics (a), and irradiation stage with MAX phase disks (b).

Fe-ION IRRADIATION OF 15-15Ti AUSTENITIC STEEL IN DIFFERENT THERMO-MECHANICAL STATES

N. Cautaerts^{1,2}, J. Pakarinen¹, R. Delville¹, Y. Yang³, M. Verwerft¹, E. Stergar¹, D. Schryvers²

¹Belgian Nuclear Research Center SCK-CEN, Mol, Belgium

²Department of Physics, University of Antwerp, Antwerp, Belgium

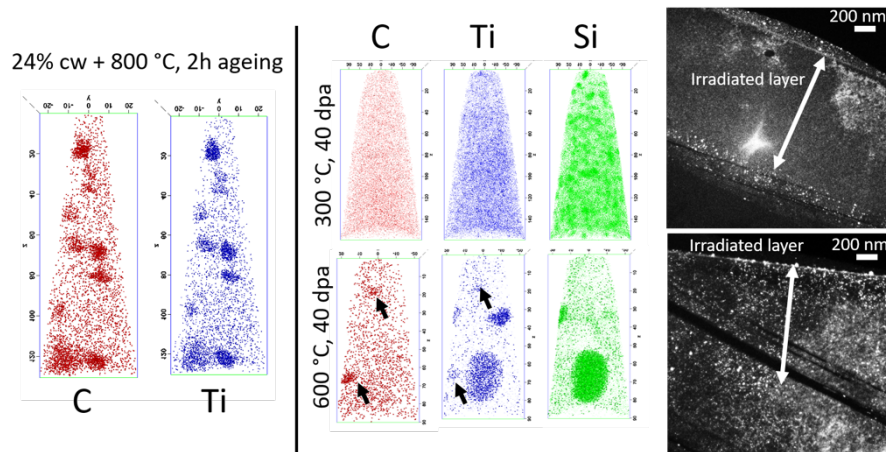
³Department of Materials Sciences & Engineering, University of Florida, Florida

Highly cold worked (15-25%) Ti-stabilized austenitic stainless steels of the 15-15Ti grade are considered prime candidate cladding materials for the first cores of several Gen IV liquid metal-cooled fast reactors worldwide. The main microstructural feature distinguishing 15-15Ti from 316L steel is the formation of TiC nanoprecipitates at high in-pile temperatures. The precipitates tend to nucleate on dislocations and act as recombination centers of interstitials and vacancies and as pinning points for dislocations, improving both swelling and creep resistance.

In sodium reactors, the fuel cladding reaches temperatures between 450 and 650 °C. In newer reactor concepts (e.g. lead-bismuth-cooled ADS), cladding temperatures only reach 300-450 °C. The behavior of 15-15Ti under irradiation at low temperature has yet to be explored. There are concerns that TiC precipitates are unstable at low irradiation temperatures and dissolve or never form. To investigate the phenomenon, 15-15Ti cladding material in different thermomechanical states was irradiated at different temperatures at MIBL.

So far, we have focused on characterization (by APT and TEM) of the material that was heat treated at 800°C/2h and subsequently irradiated, because it contains the nanoprecipitates before irradiation. Preliminary results indicate that the nanoprecipitates indeed tend to dissolve at low irradiation temperatures whereas at higher temperatures the nanoprecipitates appear more stable. At all irradiation temperatures, Ti tends to cluster with Si and Ni, but at 600 °C these clusters are much larger and seem to form well defined precipitates.

This work was supported by the U.S. Department of Energy, Office of Nuclear Energy under DOE Idaho Operations Office Contract DE-AC07-051D14517 as part of a Nuclear Science User Facilities experiment.



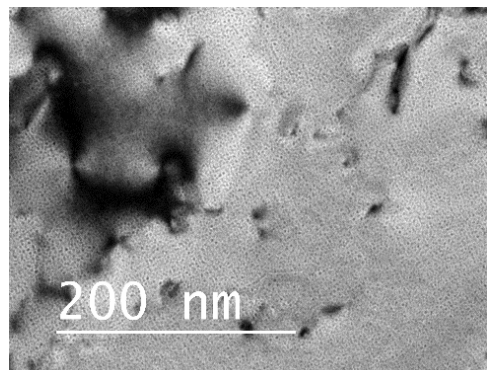
On the left, an APT measurement on non-irradiated heat treated material showing the TiC nanoprecipitates. On the right, APT on material irradiated at 300 °C shows the absence of TiC and instead fine Si clusters possibly in combination with some Ti. TEM confirms the absence of Ti-C in the irradiated layer. Irradiation at 600 °C keeps some nanoprecipitates intact and results in the formation of large Ti-Si clusters. TEM shows there are still plenty of precipitates within the irradiated layer (appearing as white spots in dark-field).

THE WINDOW OF GAS-BUBBLE SUPERLATTICE FORMATION IN BCC METALS

C. Sun
Idaho National Laboratory

The formation of helium bubbles leads to a microstructural evolution where helium bubbles usually cause hardening and embrittlement, degrading the mechanical properties of fuel cladding of fission reactors and the first-wall materials of fusion reactors. Managing the helium bubbles formation and transforming them from a liability into an asset in a controllable way will help us tailor the microstructure of nuclear materials and precisely predict the materials performance in nuclear reactors. Gas-bubble superlattice (GBS) have been observed for decades, they can form either by gas ion implantation or by nuclear transmutation. Although many possible GBS formation mechanisms have been proposed previously, a clear understanding is still missing. Fundamental understanding on the GBS formation in metals is critical for their further engagement in nuclear energy systems.

Helium ion implantation experiments were performed on tungsten in Michigan Ion Beam Laboratory. The tungsten TEM foils and bulk samples were electropolished at Idaho National Laboratory. The microstructure characterization of irradiated tungsten was also performed at Idaho National Laboratory. The figure shows the microstructure of helium irradiated tungsten under over-focusing imaging condition at zone axis of [001]. The He gas bubble superlattice is clearly formed with a well bubble alignment on {011} planes and the average diameter of helium bubbles is ~ 1.3 nm.



TEM micrograph of helium-implanted tungsten under over-focusing imaging condition.

Helium ion implantation under different conditions were performed in tungsten to determine the formation window of GBS in tungsten. Totally seven batches of samples were irradiation at temperature from 350 to 650°C, fluence from 6×10^{16} to $2 \times 10^{17}/\text{cm}^2$ with flux from 9×10^{11} to $6.2 \times 10^{12}/\text{cm}^2/\text{s}$. Temperature, fluence and flux dependent bubble lattice constant and bubble size were studied using TEM and synchrotron scattering. Our study will provide fundamental understanding on the mechanism of GBS formation in irradiated materials, which is crucial for the development of advanced nuclear materials with desired properties in a controllable way.

This work is supported by the U.S. Department of Energy under grant DE-AC07-05ID14517 and NSUF rapid turnaround proposal award #: 17-846.

Table 1 Helium on irradiation conditions of tungsten.

Batch #	Ion energy (keV)	Temperature (°C)	Fluence (ions/cm ²)	Flux (ions/sec/cm ²)
1	40	650	1×10^{17}	6.2×10^{12}
2	40	500	1×10^{17}	6.2×10^{12}
3	40	350	1×10^{17}	6.2×10^{12}
4	40	500	1×10^{17}	2.7×10^{12}
5	40	500	1×10^{17}	9.0×10^{11}
6	40	500	2×10^{17}	2.7×10^{12}
7	40	500	6×10^{16}	2.7×10^{12}

USING ION IRRADIATION TO EXTEND THE DAMAGE LEVEL OF NEUTRON IRRADIATED STAINLESS STEELS

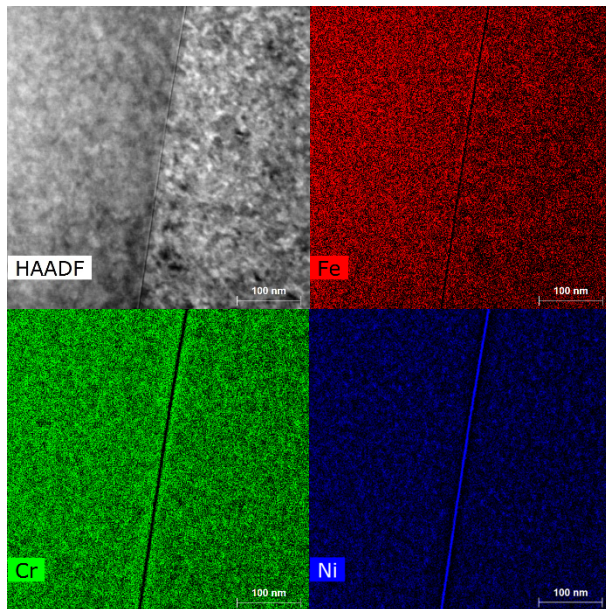
S. Levine, Z. Jiao, G. Was

Department of Nuclear Engineering & Radiological Sciences, University of Michigan

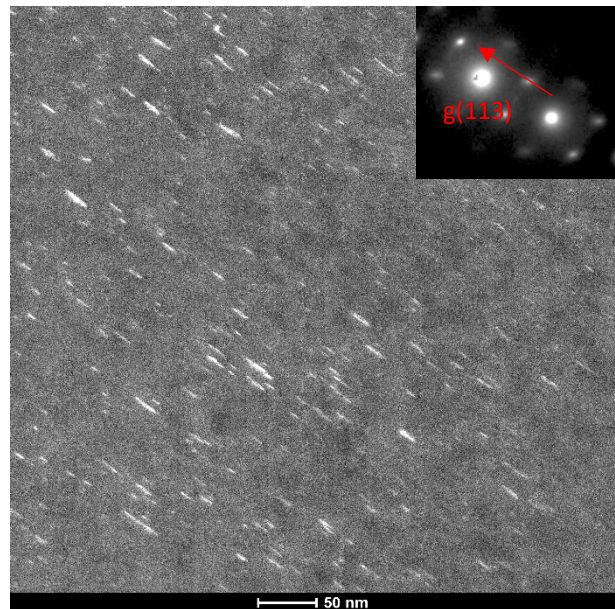
As the United States' light water reactor fleet continues to age, many plants are applying for license renewal. For regulators and plant operators, structural material degradation is a chief concern. While ion irradiation is a useful tool to predict future material degradation, resulting microstructures are extremely sensitive to initial composition and heat treatment. Unfortunately, unirradiated material of the same heat already being used in reactor is rarely available. Thus, the objective of this study is to determine the efficacy of irradiating neutron irradiated material (preconditioned samples) with heavy ions to simulate high dpa level damage.

A sample of a 304L stainless steel core shroud previously irradiated in the BOR-60 fast reactor at 320°C at a dose rate of 9.4×10^{-7} dpa/s ($E > 0.1$ MeV) to 5.5 dpa was further irradiated in the Michigan Ion Beam Laboratory with a defocused beam of 9 MeV Ni^{3+} ions at 380°C at a dose rate of $\sim 10^{-3}$ dpa/s to a final dose of 10.2 dpa. A comparison of dislocation loops, cavities, precipitates, and radiation induced segregation between 10.2 dpa BOR-60 samples and the ion+neutron irradiated sample was subsequently conducted.

This material is based upon work supported under an Integrated University Program Graduate Fellowship. In addition, this work is supported by the U.S. Department of Energy Nuclear Energy University Program (NEUP) and Nuclear Science User Facilities (NSUF) under grant DE-NE0008520.



Radiation induced segregation observed in the ion+neutron irradiated sample. In the top left, a high angle annular dark field image of the grain boundary region. Depletion of iron (red) and chromium (green) was observed as well as enrichment of nickel (blue).



Faulted dislocation loops observed with rel-rod imaging in the ion+neutron irradiated sample.

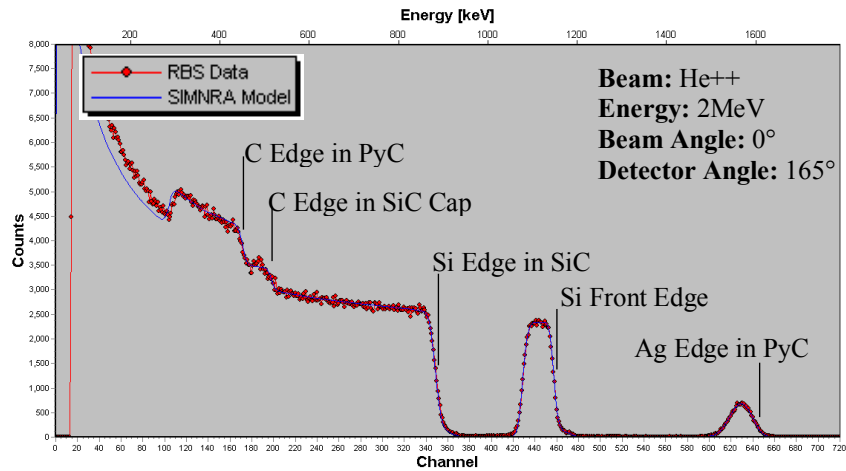
CONSTRUCTION AND CHARACTERIZATION OF SILICON CARBIDE DIFFUSION COUPLE

R. Wahlen, G.S. Was

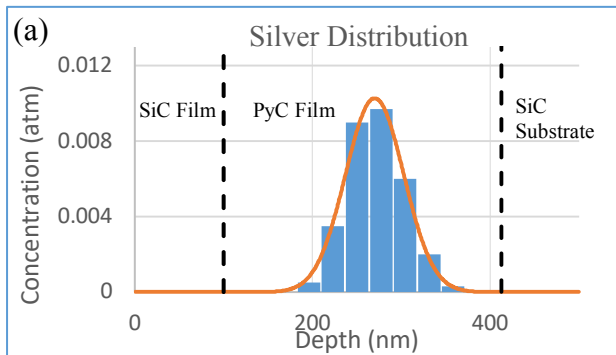
Department of Nuclear Engineering and Radiological Sciences, University of Michigan

This project focuses on identifying the mechanism for fission product transport in silicon carbide (SiC), the main component in TRISO fuel, in support of the very high temperature reactor (VHTR) fuel development. Multi-layered diffusion couples consisting of a SiC substrate, a thin pyrocarbon layer, and an SiC cap are characterized at various steps in the construction process at the Michigan Ion Beam Laboratory (MIBL). Furthermore, 400keV and 800keV implantations of silver (Ag^+ , Ag^{++}), ruthenium (Ru^+), iodine (I^+), and palladium (Pd^+) all to a target fluence of $1 \times 10^{16} \text{ a/cm}^2$ were conducted at MIBL using the implanter system. RBS analysis of a fully constructed silver diffusion couple is shown in Figure 1 while the SIMNRA model obtained by fitting to the RBS data and a Gaussian fit to the model is shown in Figure 2 as well as calculated statistics of the implanted concentration.

This research is supported by the Department of Energy under NEUP.



Measured RBS spectrum from silver implanted high temperature diffusion couple and SIMNRA.



(b)

Peak Concentration (atm%)	1.02
Peak Range (nm)	270
σ (nm)	32.8
FWHM (nm)	77.3
Integrated Implanted Fluence (a/cm^2)	9.3E+15

SIMNRA model (blue) of implanted silver concentration from RBS analysis on silver implanted diffusion couple and a Gaussian fit (red) to the model (a). Statistics from the Gaussian fit of the silver concentration (b).

Non-NSUF projects

COMPLEX CONCENTRATED ALLOYS FOR REDUCED ACTIVITY APPLICATIONS

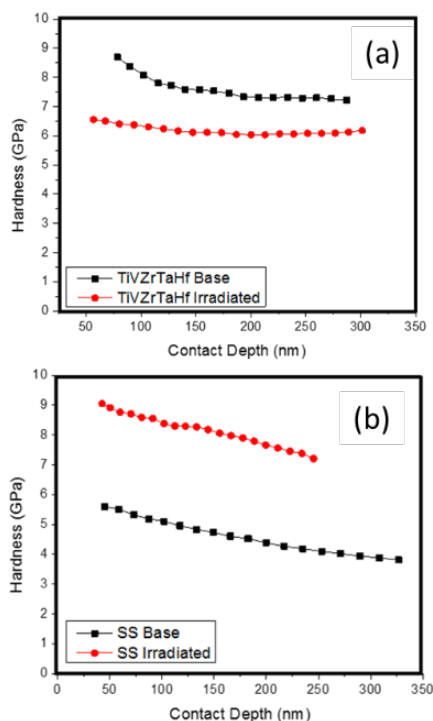
A. Ayyagari, S. Mukherjee

Department of Materials Science and Engineering, University of North Texas

This work is supported by U.S. Department of Energy, under the SBIR/STTR Contract # DE-SC0017138

The full potential of next generation nuclear reactors demands availability of radiation-resistant alloys that have long creep life and can sustain molten-salt cooled environments with temperatures in the range of 400 to 850°C. State of the art alloys require hundreds of years for the induced radioactivity to lower to “hands on level”. Some of these alloys include reduced activity ferrite martensite (RAFM) steels, 9Cr-W-V-Ta steels, V alloys, and SiC reinforced composites. An expanded alloy design strategy based on concepts of “high configurational entropy” was adopted to stabilize microstructures. Accelerated alloy development by high-throughput combinatorial technique was combined with integrated computational modeling to engineer microstructures suitable for Generation IV environment.

A series of alloys were developed from a palette of refractory elements. Among the developed compositions, the Ti-V-Zr-Ta-Hf was observed to have excellent properties. The alloy possessed a hardness of 6.5 GPa at room temperature, which was retained up to 300 °C. The modulus was 106 GPa at room temperature, and 110 GPa at 300 °C. The alloy had a cast dendritic structure with simple BCC crystal structure. The alloy was chosen for evaluating irradiation damage resistance when bombard with Ni⁺⁺ heavy ions. Irradiation experiments were carried out on Maize and beam line 7 at the Michigan Ion Beam Laboratory. Irradiation experiments were carried out at room temperature, with an integrated fluence of 1.08×10^{17} ions/cm². The beam energy was 4.4 MeV at an average sample current of 0.75 μ A.



Hardness measurements were made of the irradiated samples, which showed irradiation induced softening in contrast to a co-irradiated counter SS304 sample as shown in *Figure 1a* and *Figure 1b* respectively. TEM lift outs were made from the surface into the sample to a depth of $\sim 5 \mu\text{m}$ to assess damage as shown in *Figure 2a*. The TEM diffraction patterns shown in *Figure 2b and c* reveal a fully amorphous region at a depth of 1 micron, where maximum damage accumulated was predicted by SRIM analysis.

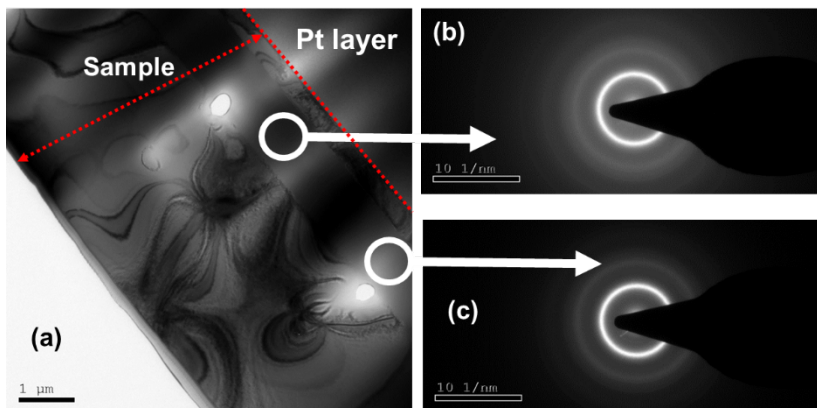


Figure 1. (a) Irradiation induced hardening on SS304 (c) Decrease in hardness after irradiation on Ti-V-Zr-Ta-Hf alloy.

Figure 2. (a) FIB Lift out showing the Pt layer, and the sample. Location of TEM diffraction are highlighted. (b) and (c) show ring patterns that correspond to amorphous regions under the Pt deposition.

CHARACTERIZATION OF COLLOIDAL NANOCRYSTAL ASSEMBLIES

S. Shaw¹, X.C. Tian¹, P. Mohapatra¹, T. F. Silva², C. Rodrigues², F. Naab³, J. Bobbitt⁴, D. Mendivelso-Perez⁴, F. Peiris⁵, J. Hay⁶, B. Yuan^{1,7}, J. J. Chang¹, M. Panthani⁷, E. A. Smith^{4,8}, L. Cademartiri^{1,7,8}

¹Department of Materials Science & Engineering, Iowa State University

²Instituto de Física, Universidade de São Paulo

³Michigan Ion Beam Laboratory, University of Michigan

⁴Department of Chemistry, Iowa State University

⁵Department of Physics, Kenyon College

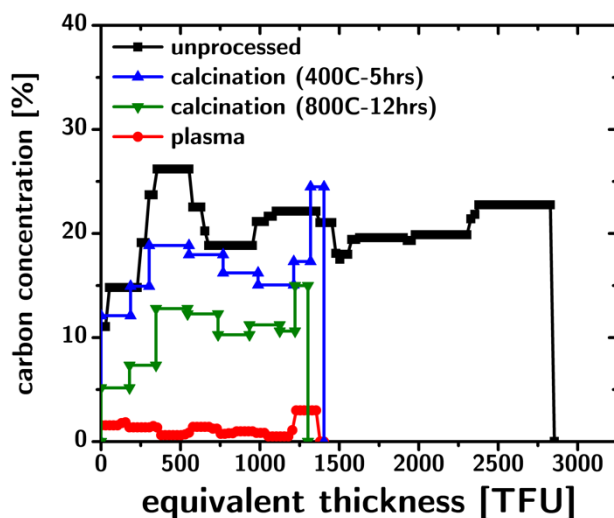
⁶Nanomechanics, Inc.

⁷Department of Chemical & Biological Engineering, Iowa State University

⁸Ames, Laboratory

This work was supported by Intel Corporation under award No. 2015-IN-2582

We have conducted a large set of experiments to characterize the influence of plasmas on colloidal nanocrystal assemblies. The removal of ligands from these assemblies is one of the most crucial limitations to this applications in devices and catalysts. The most common approach to the removal of organics from nanostructured materials is calcination. Characterization of the carbon after calcination is usually performed by FTIR, or Raman, which indicate that the organics can be effectively removed. IBA characterization is essential in this case: we showed in a recent publication that calcination leaves behind a significant amount of carbon, which is severely dehydrogenated and is therefore nearly invisible by FT-IR, Raman, or XRD characterization. These findings (Figure) are crucial to validate plasma processing as the only effective approach to the complete removal of organics from colloidal nanocrystal assemblies (CNAs) and to correct a long-standing assumption in materials chemistry (the effective removal of organics by calcination), which is the basis of several thousand papers.



Carbon depth profile in CNAs processed by calcination and plasma.

Furthermore, our extensive characterization has allowed to shed light on the influence of ligand composition on the composition of the solid-solid interfaces in the CNAs after plasma processing. IBA, and the analysis of the data allowed to obtain quantitative information about the composition of the film, the porosity, and the amount of adventitious contaminants in the pores (e.g., water). RBS is the only way we could get such accuracy, sensitivity, depth profiling, and penetration in the characterization of these films.

A number of papers that center around the results obtained at MIBL are approaching submission and dealing with various aspects of plasma processing of CNAs.

MEASUREMENT AND MODELING OF NANOCURIE LEVEL PROTON-ACTIVATION IN ZIRCONIUM ALLOYS

J. J. Carter, D. Moran, R. W. Smith
 Naval Nuclear Laboratory, West Mifflin, PA

Proton bombardment is an important technique for creating irradiation damage while producing only extremely low levels of residual activity. Although usually quite small, the degree of activation and the half-lives of the resulting radionuclides are sensitive functions of proton energy and the alloy/impurity content of the target, and for this reason it is desirable to develop a computational model to predict activation and decay in these experiments. Such a model can be used to estimate total activity and cool-down times prior to irradiation, and potentially also to identify very trace levels of impurities or contaminants in sample materials by comparison with post-irradiation gamma spectroscopy.

The purpose of the present work is to develop and experimentally validate a computational model of activation and decay in zirconium-based alloys. Rate equations for transmutation and decay reactions are used along with standard nuclear data tables, and then integrated over decreasing proton energy from the sample surface up to the maximum depth of penetration. Model predictions were calculated for alloy chemistries appropriate to both Zircaloy-4 and Zr-2.5Nb and compared to gamma spectroscopy measurements made on samples bombarded to 1 DPA with 2 MeV protons at the MIBL. Gamma spectroscopy measurements were done out to 2 years following proton irradiation. Results showed relatively good agreement between model predictions and gamma spectroscopy measurements for many long-lived isotopes. Some disagreement was seen in certain isotopes, particularly Co-57, but these differences are likely due to the lack of accuracy in the cross-section data as there exists a large disagreement between different nuclear models at these proton energies. One conclusion of the work is that the model may benefit from a series of irradiations designed specifically to accurately assess and update activation cross sections for key isotopes and proton energies.

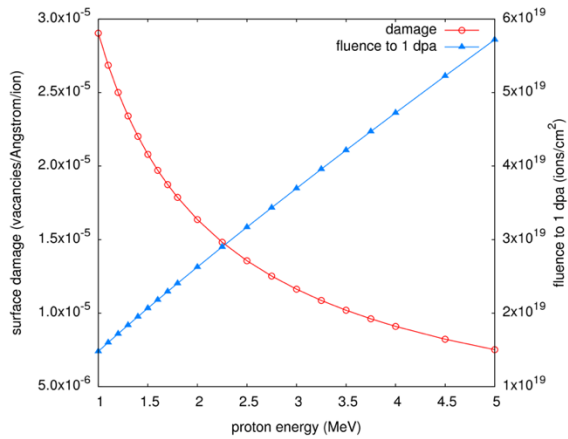


Figure 1. Damage and dose vs. proton energy.

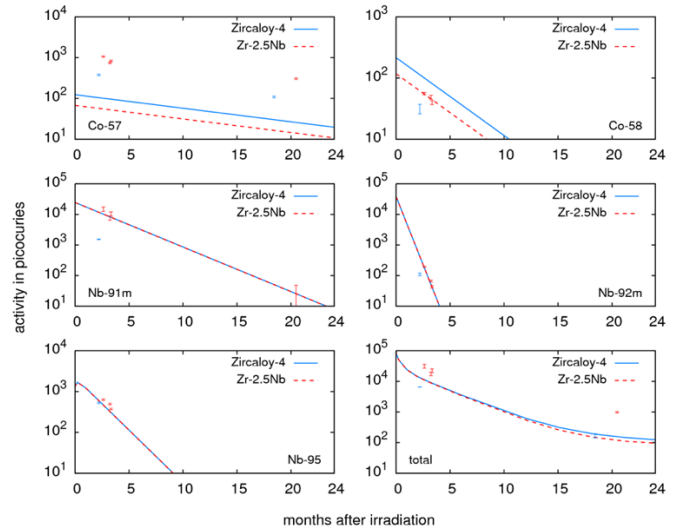


Figure 2. Activity for various isotopes as a function of time after irradiation.

IRRADIATION RESISTANCE OF SURFACE-TREATED ALLOY 718

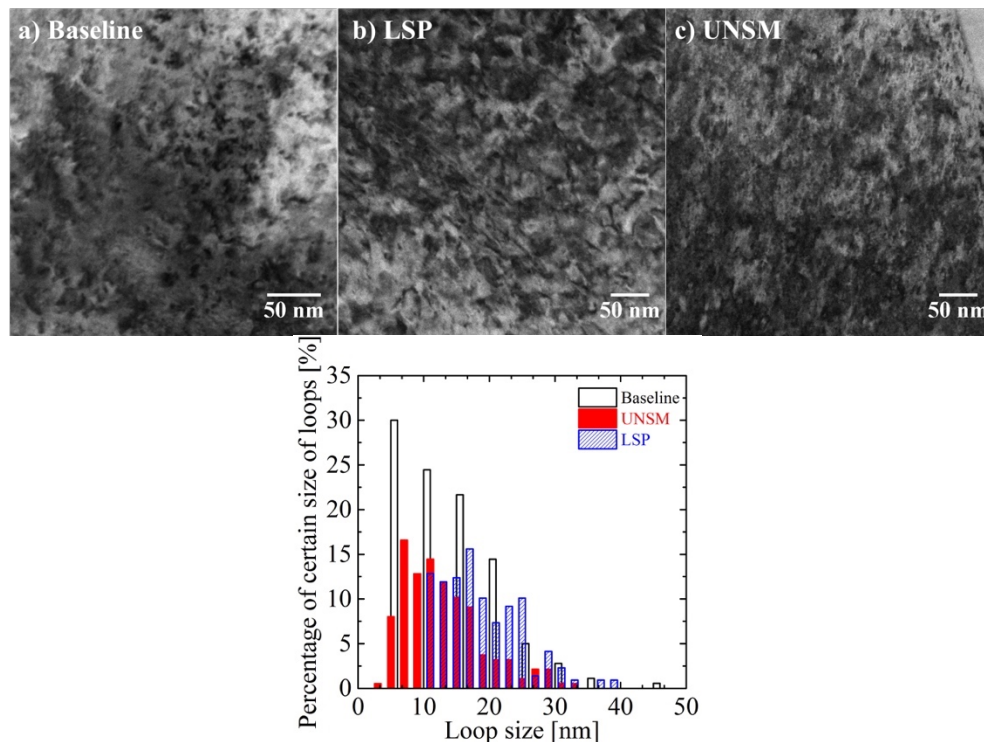
Y. Bazarbayev¹, K. Mao¹, R. Chiang², V. K. Vasudevan², J. P. Wharry¹
¹Purdue University
²University of Cincinnati

The stress corrosion cracking (SCC) of Ni-base alloys can be greatly reduced by surface treatments such as laser shock peening (LSP) and ultrasonic nanocrystal surface modification (UNSM). These techniques result in favorable compressive residual stresses, while increasing the population special coincident site lattice (CSL) boundaries, both effects of which enhance SCC resistance. However, $\Sigma 3$ coherent twin boundaries and other CSL boundaries are relatively poor sinks for irradiation defects. The objective of this work is to understand whether the improvement of SCC resistance compromises the irradiation tolerance of Alloy 718 that has undergone surface treatments such as LSP and UNSM.

Baseline (untreated), LSP, and UNSM Alloy 718 (nominally Ni-19Cr-3Mo) are irradiated with 2.0 MeV protons to 1 displacement per atom (dpa) at 500°C. Transmission electron microscopic (TEM) lamellae are prepared using focused ion beam (FIB) lift-out. Bright-field scanning TEM (BF-STEM) is used to observe dislocation loops. Through-focus TEM is used to check for bubble and void nucleation.

LSP specimens have a higher loop number density than the baseline (upper figures) due to the lower-sink-strength special grain boundaries; the loop size distribution is given for all three methods (lower figure). However, in the UNSM specimen, the loop number density is an order of magnitude lower than that in the baseline. This result suggests that the nanocrystallinity can sufficiently offset the higher population of special boundaries, enabling the UNSM specimens to be as irradiation tolerant as the baseline.

This work is supported by the U.S. Department of Energy Office of Nuclear Energy under contract DE-AC07-05ID14517, as part of Nuclear Science User Facilities project 17-922. YB is supported by the Kazakhstan JSC Center for International Programs Bolashak Fellowship.



BF-STEM images of dislocation loops of baseline, LSP and UNSM conditions Alloy 718 (upper). Distribution of dislocation loops of different sizes for each type of surface treatment (lower).

IRRADIATION EFFECTS IN WELDED ODS STEELS AT HIGH DOSE

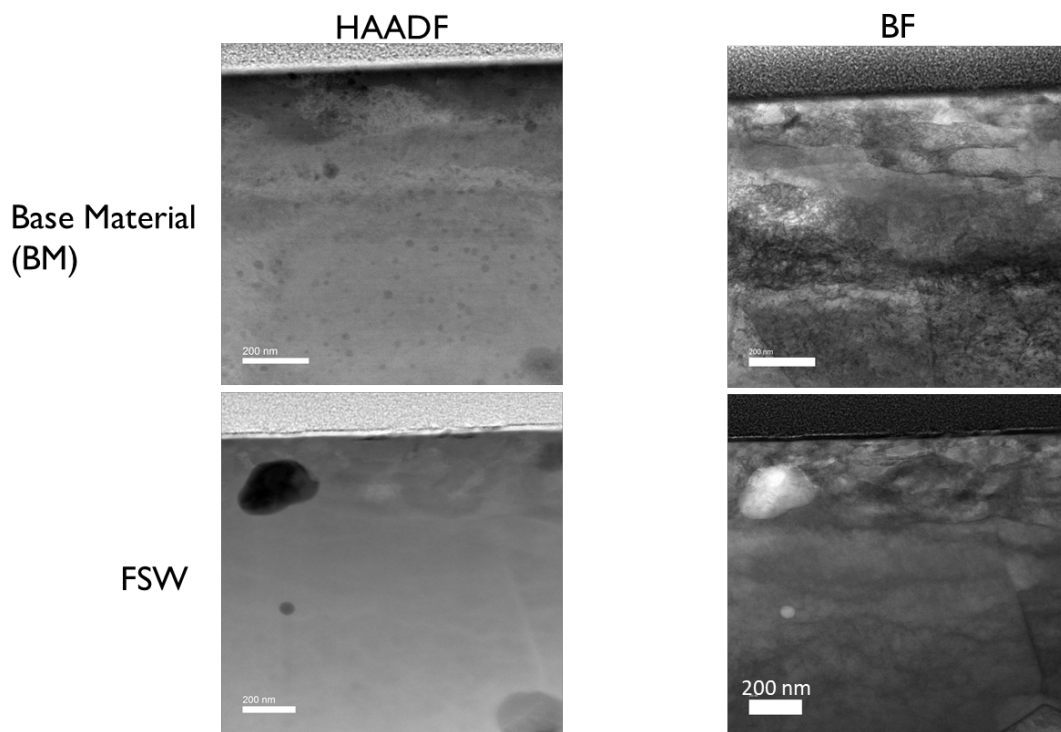
E. Getto¹, J. P. Wharry²

¹Department of Mechanical Engineering, United States Naval Academy

²School of Nuclear Engineering, Purdue University

Understanding the microstructural behavior of oxide dispersion strengthened (ODS) alloys is important for predicting the safety and structural integrity of advanced fission and fusion reactors. Furthermore, the behavior of welds in reactors is a significant concern as welds are a weak point in terms of mechanical properties. Self-ion irradiation experiments have been performed on friction stir welded (FSW) and as-received alloys MA956 to determine the microstructure response to irradiation at 450°C up to 200 displacements per atom (dpa). Irradiations were performed with 5 MeV Fe⁺⁺ ions on samples using a raster-scanned beam with a 1.7 MV Tandem accelerator at the Michigan Ion Beam Laboratory. The effects of welding and pre-irradiation microstructure were determined using an Analytic Electron Microscope in scanning transmission electron microscopy (STEM) mode and atom probe tomography (APT) was performed to determine precipitate behavior.

This work is supported by the U.S. Nuclear Regulatory Commission Grant NRC-HQ-84-14-G-0056.



Microstructure of base material and after welding in ODS alloy in MA956 imaged using STEM in the HAADF (high angle annular dark field) and BF (bright field) imaging conditions.

EFFECT ON IRRADIATION ON THE CORROSION OF 316L STAINLESS STEEL

R.D. Hanbury, G.S. Was

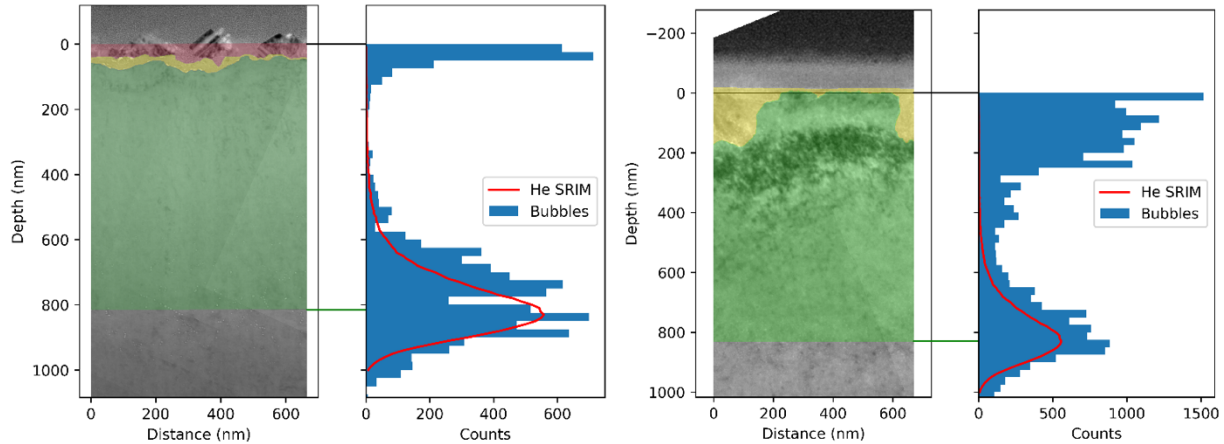
Department of Nuclear Engineering and Radiological Sciences, University of Michigan

Two *in situ* proton irradiation corrosion exposures of 316L heat 626032 were completed and samples characterized this year using the Wolverine 3 MV tandem accelerator on beamline 3. Both experiments had the following exposure conditions: 7×10^{-7} dpa/s, ~ 700 kGy/s, 320°C , 13.1 MPa, in 3 wppm H_2 water for 24 hr. The samples used the design developed in the previous year: a precipitation hardened steel backing disc (17-4 PH) was used to minimize deformation and a proton energy of 5.4 MeV was selected to reduce activity. One sample was hot-implanted with helium at 550°C to 10^{16} He/cm² before exposure to produce a bubble marker layer for measuring oxide dissolution after exposure. Results from this marker layer experiment show measurable dissolution in the irradiated region and no measurable dissolution in the unirradiated region indicating radiation induced oxide dissolution.

The implanted bubble layer has a thickness of about 300 nm, and the number density histogram can be fit to a normal distribution. The original surface can be determined by following the peak bubble line through a FIB lift-out. And since the outer oxide is formed by re-precipitation, any area between the original surface and the inner oxide has been dissolved.

From the characterization so far, the irradiated region has a continuous dissolution layer, whereas the unirradiated region has no dissolution, see below. Both regions had two different grain orientations examined for both inner oxide thickness and dissolution where applicable.

This research is supported by EDF contract number 8610-5920005571.



Irradiated region (above) and unirradiated region (below) cross-sectional bright field TEM image of helium implanted 316L exposed in IAC for 24 h at 7×10^{-7} dpa/s. On the left: green shows the remaining metal above the implantation line, yellow is the inner oxide layer, and red shows the dissolved metal bounded by the original metal surface. On the right: a number density histogram of bubbles matches the SRIM helium implantation profile which defines the marker line and the original surface.

QUANTIFYING RADIATION DAMAGE USING STORED ENERGY FINGERPRINTS

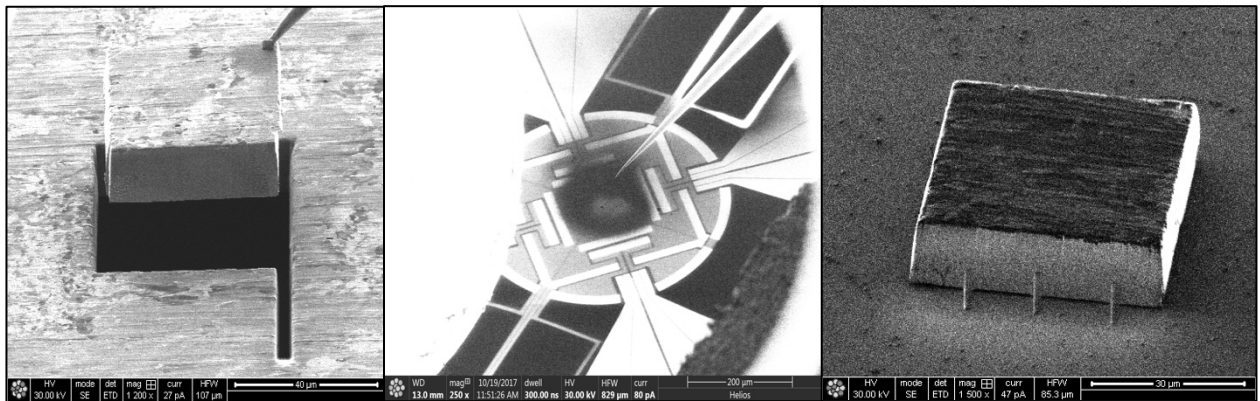
C.A. Hirst, R.C. Connick, K.P. So, P. Cao, R.S Kemp, M.P. Short
Department of Nuclear Science & Engineering, MIT

The displacements per atom (DPA), the currently accepted unit of radiation damage, does not fully capture resultant defect populations from radiation damage. Literature citing differing results with identical DPA when varying temperature, dose rate, type of irradiation, and chemical composition point to the need for a more universal and measurable unit of radiation damage. We propose to determine the remaining defect population in a material after irradiation by measuring the stored “Wigner” energy. This is the difference in energy between a sample with a defected (irradiated) microstructure and in an annealed state.

Samples are prepared using focussed ion beam (FIB) lift out from pure metal foils irradiated with He ions to a dose of 0.1 dpa at the MIBL. Fast Scanning Differential Calorimetry (FDSC) is used to heat the samples to 500C. Defects anneal out during the first run, releasing their stored energy. Subsequent runs of the annealed sample are subtracted as a baseline. Comparing these experiments to literature and collision cascade molecular dynamics simulations, the activation temperature of the energy release peaks can be matched to migration energy of a certain defect type. The integral of the peak can be divided by the formation energy of this defect to determine the number and density of defects (of a given size).

The objective of this work is to develop a technique to determine the full defect distribution in the material. From this, the processes behind defect formation and recovery will be investigated, advancing fundamental science. Knowledge of the full defect distribution in a material allows a mechanistic determination of its properties through existing models and structure-property relationships. Understanding how these defects evolve will allow more accurate predictions of material properties over time.

This work was supported by NSF CAREER Grant No. DMR-1654548, and in part by the Consortium for Verification Technology under Department of Energy National Nuclear Security Administration Award DE-NA0002534.



Scanning Electron Microscope images of the FIB sample preparation procedure. Lift out of samples from ion-irradiated foils before transfer onto Mettler Toledo UFS1 chips. Experiments are yet to be run on ion-irradiated foils and are currently being conducted on cold-worked foils with dislocations as an analogue for radiation damage.

STATISTICAL AND QUANTITATIVE EVALUATION OF GRAIN BOUNDARY PROPERTIES ON INTERGRANULAR CRACKING OF IRRADIATED MATERIAL TESTED IN SIMULATED PWR ENVIRONMENT

M. Herbst, R. Kilian, N. Huin
FRAMATOME

The main objective of the SOTERIA project is to enable nuclear power plant operators, as well as regulators, to better understand and thereby predict the ageing phenomena occurring in reactor pressure vessels and internal steels in order to ensure a safe long-term operation of existing European nuclear power plants. SOTERIA will thus provide further knowledge and tools to manage the ageing of nuclear power plants.

The WP4 aims at better understanding the influence played by the environment on internals IASCC susceptibility with particular focus on the

- Characterization of irradiation effects on microstructural evolution, including:
 - Radiation-induced segregation (RIS),
 - Creation and distribution of helium bubbles,
 - Clear bands,
- Characterization of cold work (CW) effects on oxide morphology and composition
- Determination of effects on environmental transients on oxidation
- Effects of irradiation on Stress Corrosion Cracking (SCC)

Results revealing clear trends with respect to irradiation, loading, environment and material condition as well as statistically significant results will be feed into the models being developed in another work package.

In the subtask WP4.4, the 316L material of interest was characterized prior to the 5 dpa proton irradiation performed at the MIBL. After this irradiation step, the various plates will be exposed in a 4PB condition to perform SCC initiation tests on the irradiated surface of the material. The specimens will be sent to MIBL for characterization of the material surrounding the cracks by FEG-SEM/EBSD, Analytical TEM and other techniques to assess the crack morphology, presence of epsilon or alpha-prime martensite, and associated deformation structures. These results will be compared with the results of preliminary tests performed in the same manner on non-irradiated material.

This work is supported by the EC SOTERIA Program.

INFLUENCE OF SURFACE RECONSTRUCTION ON ATOMIC ORDERING IN GaAsNBi ALLOYS

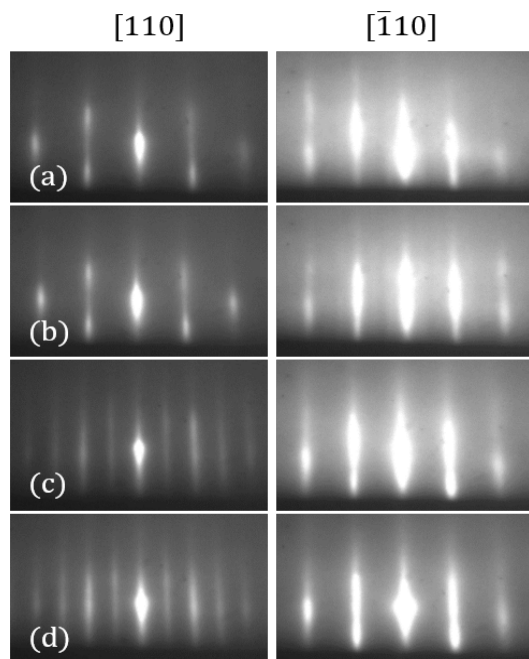
J. Occena¹, T. Jen¹, A. G. Norman,² R.S. Goldman¹

¹Department of Materials Science and Engineering, University of Michigan

²National Renewable Energy Laboratory, Golden, Colorado 80401, USA

Highly mismatched semiconductor alloys formed by incorporation of small concentrations of nitrogen or bismuth are being pursued for optoelectronic applications in the near- and mid-infrared due to the significant bandgap reduction induced by N or Bi. For example, N is proposed to interact with the GaAs conduction band, leading to a rapid lowering of the conduction band edge with increasing N mole fraction in GaAs_{1-x}N_x alloys. Similarly, Bi is proposed to interact with the GaAs valence band, leading to a dramatic bandgap reduction with increasing Bi mole fraction for GaAs_{1-y}Bi_y alloys, primarily through a lifting of the valence band edge. Thus, co-incorporation of these solute atoms to form the quaternary alloy GaAs_{1-x-y}N_xBi_y is predicted to offer a versatile material system for bandgap engineering in which the bandgap, band offsets, and strain can be independently controlled through proper balance of the N and Bi mole fractions. Here, we examine the role of surface reconstruction on long-range atomic ordering in GaAsNBi alloys. We identify a threshold substrate temperature and a range of bismuth fluxes (bismuth fractions determined using RBS) for which the surface reconstruction transitions from a (1x3) to (2x1) and CuPt ordering on the group V sublattice emerges. We propose a modified dimer-induced strain mechanism for CuPt ordering in which N atoms incorporate beneath surface dimers and Bi atoms incorporate between dimer rows. We further hypothesize that the ordered GaAsNBi alloy consists of alternating Bi-rich (N-poor) and Bi-poor (N-rich) {111}B planes, with a fraction of N atoms sharing As lattice sites as (N-As)_{As}.

This work is supported by the National Science Foundation (Grant No. DMR 1410282) and the U.S. Department of Energy Office of Science Graduate Student Research (SCGSR) Program.



Reflection high-energy electron diffraction (RHEED) patterns collected along the $\langle 110 \rangle$ directions for GaAsNBi layers grown at substrate temperature (a) 260°C, (b) 300°C, (c) 340°C, (d) 380°C. A (1 x 3) pattern observed at 260°C and 300°C transitions to a (2 x 1) pattern for 340°C and 380°C.

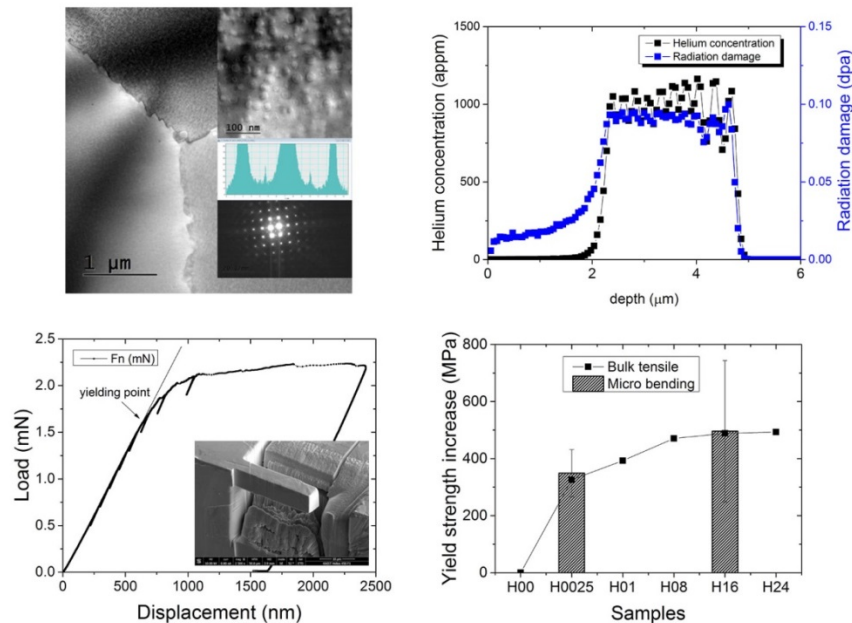
EVALUATION OF MECHANICAL PROPERTY CHANGE OF HELIUM IMPLANTATED NI ALLOY

H-H. Jin, I. S. Rye, J.H. Kwon, G.G.Lee

Nuclear Material Research Division, Korea Atomic Energy Research Institute

The objective of this work is to reveal helium bubble effect on change in mechanical property of nuclear structural materials. Target material in this work is Inconel X-750 alloy which has been used for fuel channel annular spacers in CANDU nuclear reactor. The spacer manufactured by the X-750 alloy containing high density of nanometer sized γ' phase has been known to exhibit intergranular failure after neutron irradiation, which seems to be linked with grain boundary helium bubbles. Helium implantation on commercial Inconel X-750 alloy was performed at two temperature ranges (RT and 300 °C) in the Michigan Ion Beam Laboratory (MIBL). Helium ions were used in multiple energies ranges, from 1.42 MeV to 2.82 MeV, for the development of uniform radiation damage (0.1 displacements per atom, or dpa) and implanted ion concentration (~ 1000 appm He) in the ion-implanted samples. We have established a micro-bending method for evaluation of mechanical property using small-scaled mechanical technology. Yield strength changes of unimplanted Inconel X-750 alloys were measured via the micro bending test method. Our future plan is to evaluate yield strength change of helium implanted X-750 alloys provided by MIBL. This will enhance scientific knowledge on correlation between material performance and microstructural change in nuclear structural materials.

This work is supported by a National Research Foundation of Korea (NRF) grant funded by the Korea government.



TEM image showing the γ' in X-750 alloy (top left), SRIM result showing dpa and He appm (top right)
Load displacement data obtained by micro bending test (bottom left),
Yield strength increase measured by micro bending test and bulk tensile test (bottom right)

LOCALIZED DEFORMATION AND INTERGRANULAR FRACTURE OF IRRADIATED ALLOYS UNDER EXTREME ENVIRONMENTAL CONDITIONS

D.C. Johnson¹, G.S. Was¹, B. Kuhr², D. Farkas², R. Mo³, I.M. Robertson³

¹Department of Nuclear Engineering and Radiological Sciences, University of Michigan

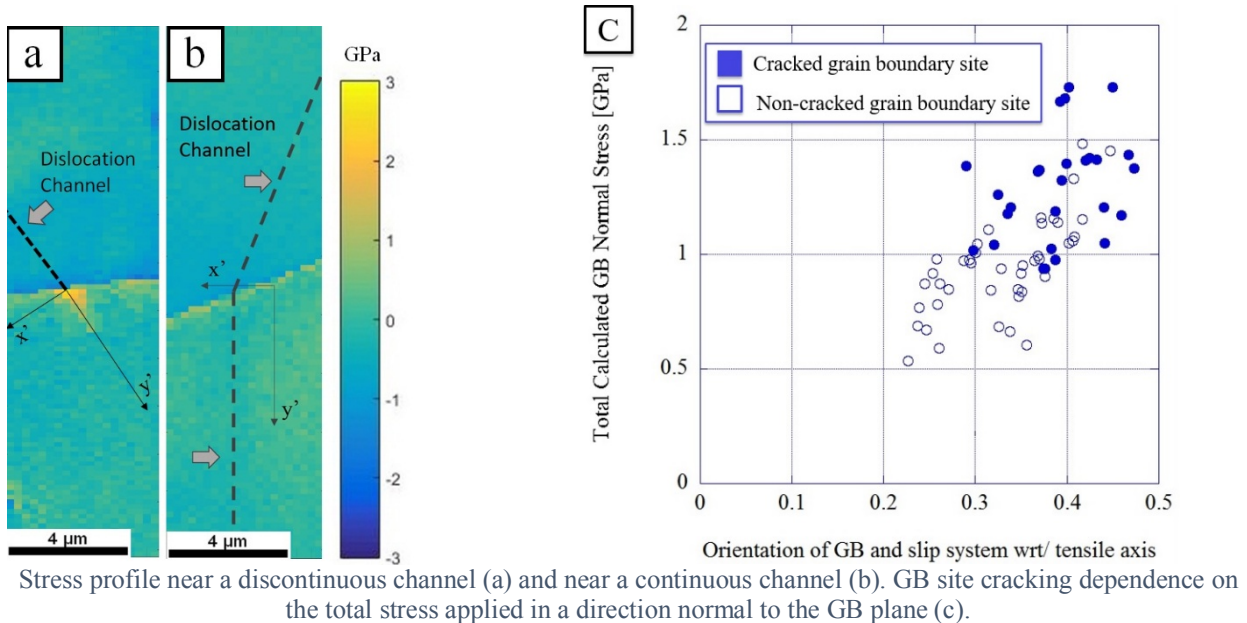
²Department of Materials Science and Engineering, Virginia Tech University

³Department of Materials Science and Engineering, University of Wisconsin

The goal of this project is to determine the role of localized deformation in austenitic steel during irradiation assisted stress corrosion cracking (IASCC). The project is a collaboration between the University of Michigan, University of Wisconsin, and Virginia Tech University with the purpose of obtaining better understanding of the mechanisms involved in IASCC. Samples are being irradiated at the University of Michigan and strained in constant extension rate tensile (CERT) tests to study the cracking behavior. Atomistic models of the experiments are being developed by Dr. Farkas' group at Virginia Tech University, and irradiated samples will be strained in-situ in a TEM by Dr. Robertson's group at the University of Wisconsin.

This year, two irradiations were performed using 2 MeV protons at 360 °C on a 13Cr15Ni lab purity alloy in the Tandem Accelerator located in the Michigan Ion Beam Laboratory. Tensile bar samples from these irradiations were used to quantify the stress component normal to grain boundaries at discontinuous dislocation channel – grain boundary interaction sites, and then related to cracking. Samples were strained in high temperature argon (288°C) to produce many dislocation channels. These channels are either arrested at the grain boundary or transmit into the adjacent grain. In both cases, residual elastic stress values were calculated using High Resolution Electron Backscatter Diffraction. Once stresses had been characterized, the samples were strained further in water, and cracking behavior was characterized, with respect to the known stress levels in the dislocation channel/grain boundary intersections. The cracking behavior of these irradiated samples show a clear correlation between the stress acting normal to the grain boundary and intergranular fracture.

This research has been supported by the Basic Energy Science office of the U.S. Department of Energy under grant DE-FG02-08ER46525.



EFFECT OF PROTON AND HEAVY ION IRRADIATION ON TRANSITION METAL DICHALCOGENIDES

T. Shi¹, R.C. Walker², J.A. Robinson², I. Jovanovic¹

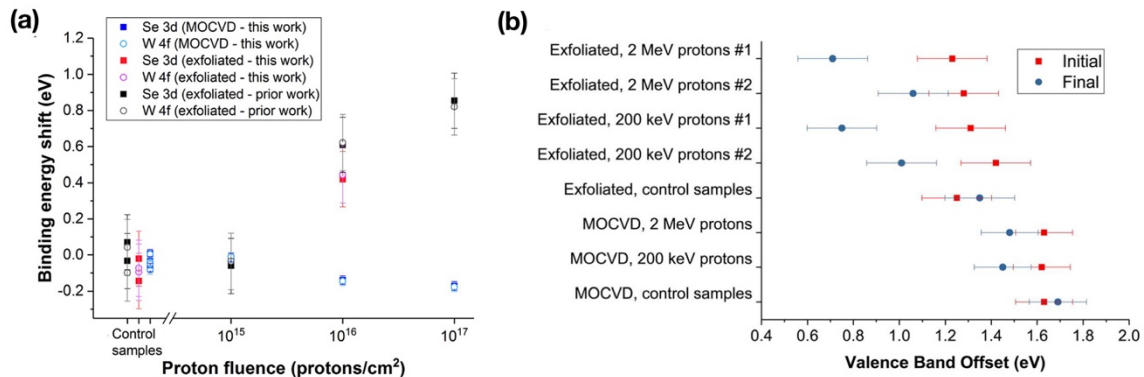
¹Department of Nuclear Engineering and Radiological Sciences, University of Michigan

²Department of Materials Science and Engineering, the Pennsylvania State University

Transition metal dichalcogenides (TMDs) have attracted significant interest in recent years due to their outstanding optical and electronic properties (sizable bandgap, high mobility, etc.) and atomically-thick dimensions. Among various TMDs, tungsten diselenide (WSe₂) with an electronic bandgap that is tunable from 1.2 eV in bulk form to 2.2 eV as a single layer has achieved particular interest due to recent progress in material growth and fabrication of ultra-thin and low-power electronics. We compared the stability against high-energy proton radiation of WSe₂ and silicon carbide (SiC) heterostructures generated by 1) mechanical exfoliation of WSe₂ flakes and by 2) direct growth of WSe₂ via metal-organic chemical vapor deposition (MOCVD). Irradiation with 200 keV or 2 MeV protons was carried out at various fluences (10¹⁵, 10¹⁶ and 10¹⁷ protons/cm²). The change of the binding energy and the valence band offset are shown in Figure (a) and (b). We found that these two fabrication techniques produced WSe₂/SiC heterostructures with distinct properties due to interface states generated during the MOCVD growth process. Both heterostructures were not susceptible to proton-induced charging up to a dose of 10¹⁶ protons/cm², as measured via shifts in the binding energy of core shell electrons and a decrease in the valence band offset. However, the MOCVD-grown material was less affected by the proton exposure due to its ultra-thin nature and a greater interaction with the substrate.

Besides the study of material damage of WSe₂, we also investigated the degradation of I-V characteristics of field effect transistors based on channeling material molybdenum sulfide (MoS₂). MoS₂ transistors were irradiated by 2 MeV protons at a fluence of 10¹⁴ ions/cm² and by 400 keV He ions at a fluence of 10¹⁴, 10¹⁵ and 10¹⁶ ions/cm². We observed a significant degradation of I-V curves at a helium fluence beyond 10¹⁵ ions/cm² and we did not observe any detectable change after exposure to 10¹⁴ protons/cm². Current experiments focus on decoupling the extent of damage of different transistor components (SiO₂ dielectric, MoS₂ channel layer, etc.).

The work related to WSe₂ material damage study was supported by the Defense Threat Reduction Agency (DTRA) under grant number HDTRA1-14-1-0037.



Binding energy shifts induced in the Se 3d and W 4f peaks of the exfoliated and MOCVD WSe₂ by exposure to 2 MeV protons at various fluences (a), Shifts in the valence band offset between WSe₂ and SiC induced by exposure to protons at a fluence of 10¹⁶ protons/cm² (b).

DUCTILITY OF COMMERCIAL AND ADVANCED ALLOYS SUBJECTED TO PROTON IRRADIATION

C. Lear, M. Wang, M. Song, G.S. Was

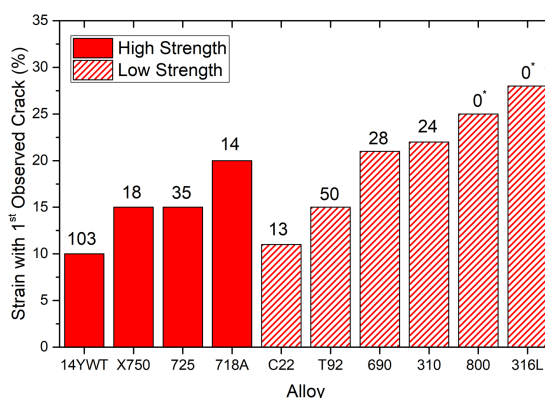
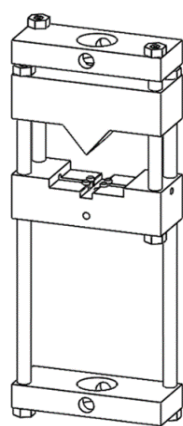
Department of Nuclear Engineering and Radiological Sciences, University of Michigan

The Advanced Radiation Resistant Materials (ARRM) program is tasked with identifying commercial and advanced alloys with superior resistance to radiation induced damage, including changes in microstructure, corrosion, and mechanical properties with irradiation. This last point has been the focus of much consideration, as the effects of accelerated testing with proton or ion irradiation are limited to depths of $\leq 50 \mu\text{m}$ below the sample surface. This year candidate stainless steels (316L, 310, 800), Ni-based alloys (690, C22, X-750, 718-A, 725), and advanced alloys (T92, 14YWT) were tested using a three-point bending method to evaluate the loss of ductility in this irradiated surface layer.

Samples were irradiated at the Michigan Ion Beam Laboratory (MIBL) to a dose of 5 dpa using a 2 MeV proton beam and an irradiation temperature of 360 °C. The irradiated samples were bent at strain rates of 2×10^{-4} using a custom holder and an MTS Alliance RT/50 mechanical testing frame. Displacement of the sample center, and thus strain, was measured using a high-resolution (0.6 μm) sensor from LORD MicroStrain in constant contact with the bending, irradiated surface. Bending was carried out in increments of several percent strain, until cracks were observed on the irradiated surface using scanning electron microscopy.

Stainless steels 316L and 800 showed the most resistance to irradiation induced ductility loss among the candidates, completely resisting cracking to the mechanical limits of the sample holder. Of those candidates which did crack, alloys 310, 690, and 718-A showed the most post-irradiation ductility; alloys C22 and 14YWT the least. Comparison to ultimate elongation data from room-temperature tensile testing of unirradiated samples revealed no clear trends in ductility loss with changes in microstructure or hardness, but testing of unirradiated samples using the same three-point method will continue into the coming year for a more definitive point of reference. It is particularly important to note, however, that even the worst performing candidates resisted cracking to at least 10% plastic strain – well beyond service conditions.

The ARRM program is supported by the Electric Power Research Institute (contracts 10002164 and 10002154) and the U.S. Department of Energy (contract 4000136101).



Drawing of the bend test holder (left). Strain at which cracks were first observed for each candidate (right). Number annotations indicate the number of cracks observed after at additional 5% plastic strain beyond those first cracks; star annotations indicate candidates which did not crack.

INVESTIGATION OF ION IRRADIATION BEHAVIOR OF NEW SILICON CARBIDE (SiC) AND NANOSTRUCTURED FERRITIC ALLOY (NFA) COMPOSITE

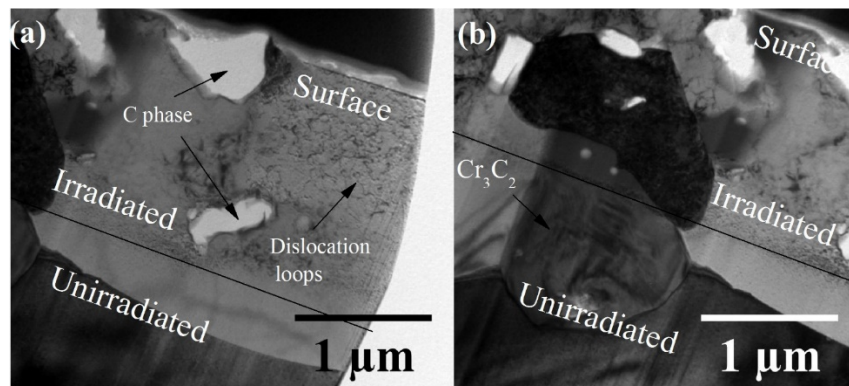
K. Ning, K. Bawane, K. Lu

Department of Materials Science and Engineering, Virginia Polytechnic Institute and State University

Nanostructured ferritic alloy (NFA) steel has been developed as a notable nuclear cladding material that possesses high mechanical strength, high temperature creep resistance, and good oxidation and irradiation tolerance for light water accidental conditions and generation IV nuclear reactor applications. SiC has strong covalent bonds, high physical and chemical stabilities and mechanical strength, as well as good irradiation resistance. In our work, SiC is introduced into the NFA matrix to create a novel SiC-NFA composites to combine the advantageous properties from each component for advanced nuclear cladding application. A $\text{Cr}_3\text{C}_2@/\text{SiC}$ -NFA composite has been developed and demonstrated clear benefits in densification and oxidation behavior. In this study, we focus on a $\text{NFA}_{\text{Si}}-\text{Cr}_3\text{C}_2-\text{C}$ composite, which is derived from the $\text{Cr}_3\text{C}_2@/\text{SiC}$ -NFA composite system, as a fundamental study of the irradiation response.

The sintered $\text{Cr}_3\text{C}_2@/\text{SiC}$ -NFA composite with a fine polished surface and 2.2 mm thickness was prepared for Fe^{++} ion irradiation, which was conducted at Michigan Ion Beam Laboratory (MIBL) of University of Michigan. A 4.4 MeV Fe^{++} beam with a controlled ion-fluence of 2.2×10^{17} ions/cm² bombarded the sample surface for 22 hrs at 43°C. After the ion irradiation, the irradiated sample surface showed an obvious dark color due to the high roughness.

SRIM simulation shows that a displacement damage up to ~ 205 dpa has been produced for the $\text{NFA}_{\text{Si}}-\text{Cr}_3\text{C}_2-\text{C}$ composite. Three phases of NFA_{Si} , C, and Cr_3C_2 are identified in the entire sample based on the transmission electron microscopy (TEM). The difference in the irradiation induced damage depth is shown in the figure. The regions with difference phase compositions have different ion irradiation induced depth. In the cases of NFA_{Si} , $\text{NFA}_{\text{Si}}+\text{C}$, and $\text{C}+\text{NFA}_{\text{Si}}$ shown in Fig. 1a, their damage depths end at 1.49 μm , 1.65 μm and 1.68 μm , respectively. In the cases of $\text{NFA}_{\text{Si}}+\text{Cr}_3\text{C}_2$ shown in Fig. 6b, the damage depth is smaller at 1.47 μm . Electron diffraction analysis shows that NFA_{Si} remains crystalline but with dislocation loops after the ion irradiation. The C phase on the sample surface is more vulnerable to amorphization but the C phase inside the sample matrix is partially amorphized. The Cr_3C_2 phase in the matrix is easily damaged and completely amorphized. These findings offer useful guidance for nuclear cladding material development.



Irradiation induced damage depth from regions with different phase compositions.

ACCELERATED IRRADIATIONS FOR EMULATION OF HIGH DAMAGE MICROSTRUCTURE IN FERRITIC-MARTENSITIC STEELS

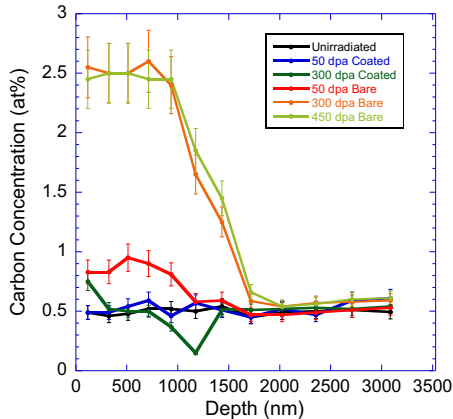
A.M. Monterrosa, Z. Jiao, G.S. Was

Department of Nuclear Engineering and Radiological Sciences, University of Michigan

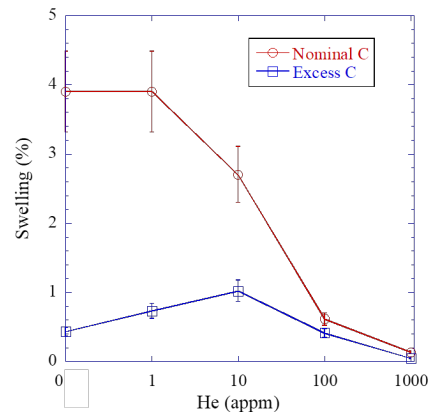
The new generation of faster reactors is seeking to push damage levels in structural materials to very high damage, in excess of 500 dpa. Using fast reactors to irradiate materials to such high damage is prohibitively expensive and time-consuming. This project will study how effectively self-ion irradiations can be used to emulate microstructural features (voids and precipitates) seen in neutron-irradiated HT9 and other ferritic-martensitic (F-M) steels.

Self-ion irradiation experiments have been performed on ferritic-martensitic alloys T91 to determine swelling behavior at 460°C, at damage levels up to 450 dpa with various levels of helium pre-implanted (0, 1, 10, 100, and 1000 atomic parts per million). The irradiations were performed using the 3MV Wolverine accelerator at the Michigan Ion Beam Laboratory. The effects of damage on void swelling were analyzed using a transmission electron microscope in scanning mode (STEM). Irradiations were performed with samples with and without alumina coatings to prevent carbon contamination. Nominal carbon samples exhibited no observable carbide formation and enhanced cavity nucleation and growth. Without an alumina coating, carbon trapped vacancies and promoted recombination resulting in a microstructure which heavily suppressed cavity nucleation. In the excess carbon samples, higher helium levels promoted a higher density of cavity nucleation. At the high helium levels of 100 and 1000 appm, swelling is suppressed due to the formation of many small cavities effectively diluting the available vacancies. Intermediate levels of helium (1 and 10 appm) show enhanced swelling due to increased nucleation, without suppressing growth. In the nominal carbon condition, this trend is not observed. High nucleation occurs in the 0 appm helium case, and further additions of helium only serve to suppress swelling. These results suggest that in highly nucleation resistant microstructures, additions of helium will result in a peaked swelling behavior. However, in a lesser nucleation resistant microstructure, helium is not needed to promote swelling and can actually cause it to decrease.

This work is supported by DOE NEUP award DE-AC07-05ID14517.



Carbon concentration as a function of depth for various damage and coating conditions obtained with NRA



Swelling as a function of helium pre-implantation level is shown for nominal and excess carbon T91 at 300 dpa.

ION-SLICED LITHIUM NIOBATE THIN FILMS

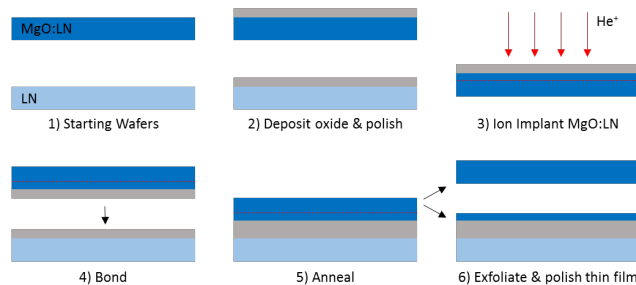
J.T. Nagy, and R.M. Reano

Electroscience Laboratory, Department of Electrical and Computer Engineering,
The Ohio State University

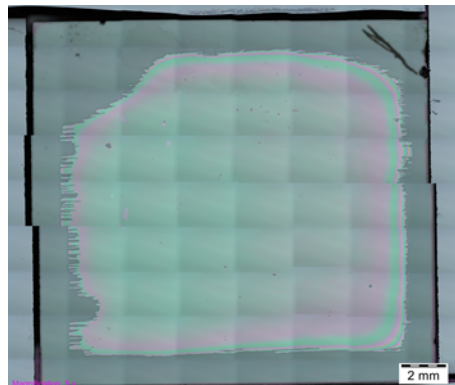
Lithium niobate (LiNbO_3) thin films with sub-micron thickness are useful for on-chip optical devices. These thin films enable high optical confinement resulting in small and highly efficient devices. The films are ion-sliced from a bulk wafer by implanting with He^+ ions, bonding to a supporting substrate, and a subsequent heat treatment. The ions form a damage layer localized at the implantation depth, which is determined by the ion energy. The heat treatment causes stress at this damage layer and causes a thin film to split off.

We started with a 3" x 1 mm thick 5 mol % magnesium oxide doped lithium niobate wafer, coated with 100 nm of silicon dioxide (SiO_2) on one surface and diced into approximately 1.5 cm samples. The samples were mounted to a 4" aluminum carrier with colloidal silver paste. The aluminum carrier was then mounted to a copper fixture provided by the Michigan Ion Beam Laboratory with doubled sided copper tape. Implantation occurred on the surface with the SiO_2 . The implant dose was $4 \times 10^{16} \text{ He}^+/\text{cm}^2$ and the energy was 250 kV. SRIM modeling predicts 250 kV will produce a 797 nm thick LiNbO_3 film. The current density was set to $0.25 \mu\text{A}/\text{cm}^2$ resulting in a total implant time of approximately 8 hrs. Thin films were successfully split and the thickness was measured with a Dektak stylus profilometer and found to be near 800 nm, in good agreement with simulations. Chemical-mechanical polishing is used to create an optically smooth surface with sub-nm roughness and thin the films to a final thickness of 700 nm.

This material is based upon work supported by the National Science Foundation under Gran No. 1436414



Fabrication process. 3-inch MgO:LN donor wafer and LN substrate (1) are coated with oxide and polished (2). Then the wafers are diced and implanted with He^+ ions at 250 keV (3). The samples are cleaned, bonded (4) and annealed (5). The annealing exfoliates the thin film which is then polished (6).



Optical microscope capture with image stitching of 700 nm thick film bonded to lithium niobate substrate.

EFFECT OF IRRADIATION ON CORROSION OF 304 NUCLEAR GRADE STAINLESS STEEL IN SIMULATED PWR PRIMARY WATER

P. Deng^a, Q.J. Peng^{a,*}, E.-H. Han^a, W. Ke^a, C. Sun^b, Z. Jiao^c

^aCAS Key Laboratory of Nuclear Materials and Safety Assessment, Institute of Metal Research, China

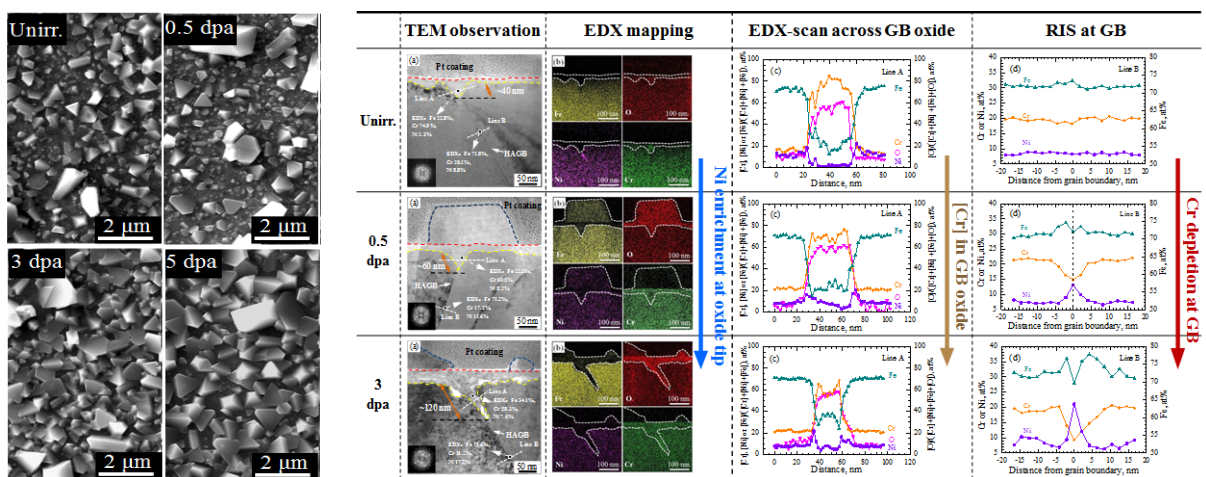
^bState Power Investment Corporation Research Institute, China

^cDepartment of Nuclear Engineering and Radiological Sciences, University of Michigan, USA

Irradiation-assisted stress corrosion cracking (IASCC) of austenitic stainless steel (SS) core components is one major concern for maintenance of nuclear power plants. Previous studies suggested that to understand further the mechanism of IASCC, attentions should also be paid on the corrosion of irradiated alloys, in addition to the localized deformation behavior. In this study, the effect of irradiation on corrosion of 304 nuclear grade SS in simulated pressurized water reactor (PWR) primary water was investigated by comparing the microstructure of the oxide scale formed on the steel irradiated to different doses by proton. The objective is to correlate the irradiation dose to the overall corrosion and localized corrosion at the grain boundary (GB).

The results revealed that increasing irradiation dose promoted both corrosion and intergranular corrosion of 304 nuclear grade SS in simulated PWR primary water. This is attributed to the promoted corrosion by irradiation induced defects and the depletion of Cr at the GB. The irradiation-induced defects are preferential sites for nucleation of oxide particles in the outer layer of the oxide scale, which led to formation of an increased number of oxide particles, as shown in the image (left). Due to Cr depletion at the primary GB in the irradiated steel, the oxide formed at the GB had a lower Cr content and was less protective than that formed at the GB in the solution annealed steel, causing a promoted intergranular corrosion by irradiation, as shown in the image (right).

This work is supported by International Science & Technology Cooperation Program of China (2014DFA50800), and National Natural Science Foundation of China (Grant No. 51571204). The authors are grateful to the Ion Beam Laboratory at the University of Michigan for performing proton implantation experiments



SEM observation of surface morphology of the oxide scales formed on 304NG SS subjected to different irradiation doses following the 500-h exposure in simulated PWR primary water at 320 °C (left).

TEM observation of the localized corrosion at a grain boundary in solution annealed and irradiated 304NG SS following the 500-h exposure in simulated PWR primary water at 320 °C (right).

REACTIVE MAGNETRON SPUTTERING OF EPITAXIAL SCANDIUM NITRIDE FOR HIGH PERFORMANCE ELECTRONICS

A.N. Reed¹, V. Vasilyev², D.C. Look³, M. Schmitt¹, H. Smith¹, H.M. Jeon¹, J.S. Cetnar², B.M. Howe¹

¹ Materials and Manufacturing Directorate, Air Force Research Laboratory, Wright-Patterson Air Force Base, Ohio 45433

² Sensors Directorate, Air Force Research Laboratory, Wright-Patterson Air Force Base, Ohio 45433;

³ Semiconductor Research Center, Wright State University, Dayton, Ohio 45435

With technological advances in electronics increasing the need for high performance devices (i.e. high power-high speed), there has recently been a surge in research in transition metal nitrides. The inherent mechanical, chemical and high temperature stability of transition metal nitrides make them ideal candidates for high-performance high-temperature electronics. Scandium nitride (ScN) is of particular interest for incorporation into gallium nitride (GaN) based electronics. Stoichiometric ScN is an n-type III-V semiconductor with a moderate band-gap (2.1-2.4 eV) and high reported carrier concentrations (up to 10^{21} cm⁻³). With its rock salt structure and lattice constant of 4.51 nm, ScN has great potential for hetero-epitaxial growth on sapphire (Al₂O₃), with a lattice constant $a = 4.78$ nm, and magnesium oxide (MgO), $a = 4.21$ nm. In addition, its close lattice match with GaN (<0.1% mismatch) makes ScN a good candidate for use as a buffer layer for hetero-epitaxial GaN on silicon (Si), in ScN-GaN heterostructures, or as an ohmic contact for GaN devices. Incorporation of ScN films into GaN devices requires high quality (i.e. low surface roughness, large grain-oriented crystals, low oxygen contamination) films.

In this work we investigate hetero-epitaxial growth of ScN films on GaN, Al₂O₃ <0001>, and MgO <100> substrates using unbalanced reactive magnetron sputtering with external electro-magnetic coils. The effect of coil current, target power and nitrogen gas fraction on film stoichiometry, microstructure and surface morphology was investigated by correlating film properties, determined through x-ray photoelectron spectroscopy, x-ray diffraction, transmission electron microscopy and atomic force microscopy, with the deposition parameters and plasma conditions during film growth. Hall measurements of the films showed that resistivity and mobility were strongly dependent on crystalline quality and ScN crystal orientation. The Hall mobility of (111)-oriented ScN films on (0001) sapphire increased from 0.95 cm²/(V*S) to 7.8 cm²/(V*S) and the resistivity decreased from 1.57×10^{-3} Ω/cm⁻³ to 6.52×10^{-4} Ω/cm⁻³ as the full width half maximum of the ScN (001) x-ray diffraction peak decreased. The transport properties of the (100)-oriented ScN were significantly better than those of the (111)-oriented films with mobilities > 80 cm²/(V-s) and resistivity < 1.77×10^{-5} Ω/cm⁻³. The RBS data from the MIBL enables us to analyze the atomic density of our films. We combine this information with measurements of the ion current at the substrate during growth to get an ion flux to metal neutral flux ratio (J_i/J_{Me}) at the substrate during growth. The ratio, J_i/J_{Me} , is an important parameter for controlling film quality.

This work is funded by the Air Force Office of Scientific Research under contract FA96550-17RYCOR490-RX.

DOSE RATE DEPENDENCE OF Cr PRECIPITATION IN IRRADIATED Fe-Cr ALLOYS

E. Reese, G. R. Odette, E. Marquis

Department of Materials Science and Engineering, University of Michigan

Ferritic/martensitic (F/M) alloys, with high Cr content, are leading candidates for nuclear reactor components because of their corrosion resistance and favorable mechanical properties. However, the evolution of F/M alloy microstructures and the corresponding degradation of their mechanical properties under neutron irradiation are a concern. One issue is the hardening and embrittlement caused by the precipitation of the α' phase observed in both model and commercial Fe-Cr alloys under varying neutron irradiation conditions.

Prior observations of α' precipitation in neutron-irradiated Fe-Cr alloys above 300 °C, are consistent with a thermodynamically driven process that is kinetically accelerated by radiation-enhanced diffusion. Small angle neutron scattering (SANS) and atom probe tomography (APT) studies of neutron-irradiated and thermally aged model Fe-Cr alloys found near equilibrium α' compositions, from 80 to 95 at.% Cr for temperature from 320 to 500 °C, e.g. However, a number of APT studies on binary Fe-Cr alloys also reported significantly lower than equilibrium Cr concentrations, down to < 50 at.% Cr, generally for smaller α' precipitates ($r < 1$ to 1.5 nm). To test the hypothesis that α' precipitation is affected by dose rate, primarily by the ballistic mixing mechanism, a series of Fe self-ion irradiations were performed, spanning three orders of magnitude in dose rate. The resulting spatial distributions of Cr were quantified using APT. The ion irradiation results were also compared to lower dose rate neutron irradiations at 320 °C.

One of ion irradiations was performed at the Michigan Ion Beam Laboratory (MIBL) using a defocused beam of 5 MeV Fe²⁺ ions to a nominal dose of 6.0 dpa at a depth of 0.5 μ m and a dose rate of 3×10^{-5} dpa/s.

Part of this work was funded by the Department of Energy Nuclear Energy University Program and the University of Michigan IRP.

AN EXPERIMENTAL TECHNIQUE FOR PRODUCING DENSE TRANSITION ALUMINA POLYMORPHS

A.L. Clauser,¹ K. Oware Sarfo,² L. Árnadóttir,² M.K. Santala¹

¹School of Mechanical, Industrial, and Manufacturing Engineering, Oregon State University

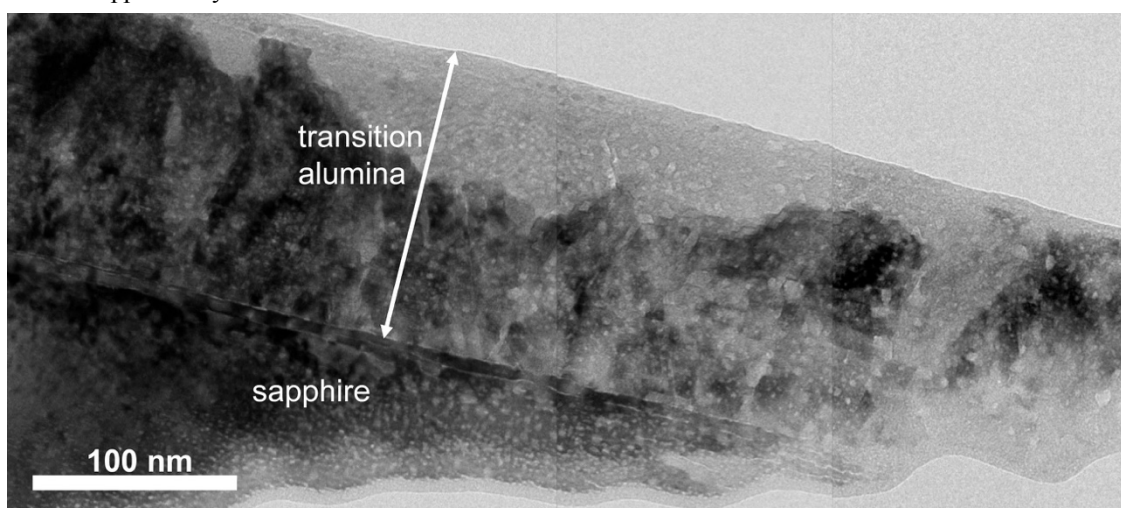
¹School of Chemical, Biological, and Environmental Engineering, Oregon State University

The thermodynamically stable form of Al_2O_3 is α -alumina (called sapphire in single crystal form), however there are many metastable transition polymorphs that can be produced by the dehydration of aluminum hydroxides and oxyhydroxides on an industrial scale. These polymorphs, especially γ -alumina, are widely used as supports in heterogeneous catalysis. The γ phase has been described as having a defect spinel structure, but details of the crystal structure, distribution of cations and vacancies on octahedral and tetrahedral sites, and even stoichiometry are the subject of debate. Structural variation may result from diverse precursors and processing paths used to produce γ -alumina, resulting in variable purity, crystallinity, ordered domain size, specific surface area, and residual hydroxylation. Michigan Ion Beam Laboratory resources were used to create a model experimental system for the study of the structure of transitional alumina, including γ -alumina.

A 1" \times 1" sapphire wafer was sequentially implanted with $4 \times 10^{16} \text{ cm}^{-2}$ Al at 90 keV and $6 \times 10^{16} \text{ cm}^{-2}$ O at 55 keV. The energies were chosen to achieve overlap in the implantation profile and the 2:3 ratio was intended to maintain the stoichiometry to the degree possible. The high fluences and liquid nitrogen cooling during implantation resulted in the amorphization of a near surface layer of the sapphire. The wafer was sectioned, and pieces were annealed at different temperatures to produce dense transition alumina. Annealing at 800°C for 25 h resulted in a 140 nm surface layer of a dense transition alumina (see figure). X-ray and electron diffraction showed this surface layer of transition alumina has a crystal structure consistent with γ -alumina, which was the desired outcome.

The transition alumina produced by this method has few impurities, limited only by the impurity level of the sapphire, and have a strong texture due to topoxially growth of the transition alumina from the sapphire. These properties were desired for transmission electron microscopy studies of the structure of transition alumina and their interactions with catalytically active metals.

This work is supported by the National Science Foundation under Grant No. 1610507.



A composite of three transmission electron micrographs showing a cross section of a sapphire wafer implanted with high fluences of Al and O, then thermally annealed in air for 25 h at 800°C. The implantation amorphized the near surface layer of the sapphire, which re-crystallized as a transition alumina. Such materials are being used in fundamental studies of the structure of transition alumina and their interactions with catalytically active metals.

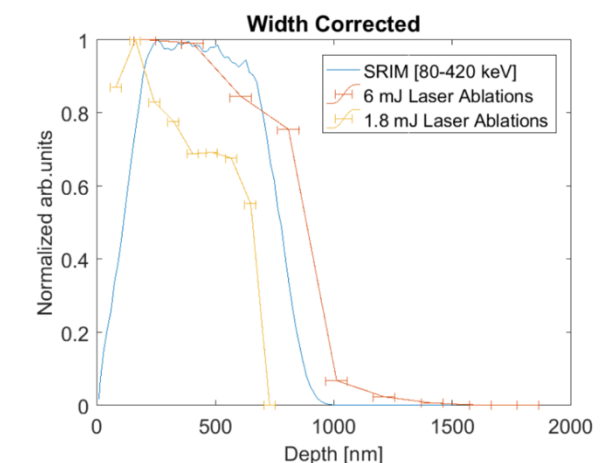
THE CALIBRATION OF LASER-BASED SURFACE CHARACTERIZATION TECHNIQUES

G. Shaw, X. Hu, B.D. Wirth
University of Tennessee – Knoxville
Oak Ridge National Laboratory

The fusion community chose tungsten (W) as the material to construct ITER's divertor. They chose W due to its high melting point, low sputtering yield, and high thermal conductivity. However, when tungsten is exposed to extreme conditions such as high ion energies and temperatures surface and bulk modifications in the plasma facing component (PFC). The PFC will undergo blistering, erosion, and retention that can have detrimental effects on the material and the bulk plasma properties. The motivation for conducting these experiments is to investigate fuel retention using a newly developed technique to quantify gas retention as a function of depth. The impact of this study demonstrates total fuel retention and provides experimental data necessary for the validation of computational models.

Simultaneous Laser Ablation Mass Spectroscopy (LAMS) and Laser Induced Breakdown Spectroscopy provide depth-resolved identification of He implanted in a polycrystalline tungsten (PC-W) target. The implantation profile was specifically designed as a calibration method to relate mass concentration to spectral intensity as a function of depth. The He implantations were performed at energies from 410 keV – 80 keV to form an approximately flat concentration profile, ~200 appm He, over a depth range 0.30 – 1 microns.

Six PC-W specimens were shipped to The University of Michigan Ion Beam Laboratory for He ion implantation. The helium implantations were performed at energies from 410 keV – 80 keV to form an approximately flat concentration profile, ~200 appm He, over a depth range 0.30 – 1 microns. The 6 specimens are now reference materials for calibrating the LIBS-LAMS station. LIBS measures the spectral intensity of the analyte and major element in the material, which is He and W respectfully. This is only a qualitative measurement because spectral intensity, or the integration of the spectral peak, is not directly proportional to the atomic concentration. However, performing LIBS on a reference material that has a known concentration of the analyte at a known depth can provide a calibration function and quantifiable analyte results. Similarly, LAMS will use the reference material to calibrate the QMS by measuring the He



mass concentration as a function of depth and comparing it to the expected concentration depth profile. LAMS was performed on one of the reference materials and the results are still being interpreted. However, the first qualitative analysis is promising. As shown in the figure, the SRIM and two experimental measurements have been normalized to show a qualitative comparison of He as a function of depth. In first experiment was performed at 6 mJ (red) and the second experiment at 1.8 mJ (yellow) and the SRIM range profile in black. The 6 mJ profile compares well while the 1.8 mJ intensity is significantly lower. The reasons for why the 1.8 mJ is lower is still being investigated.

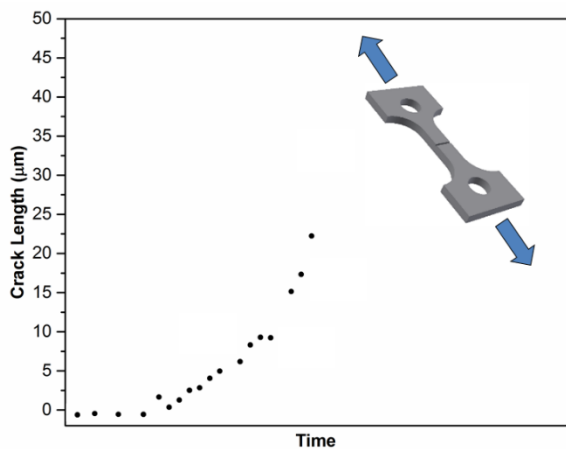
Normalized plot comparing the SRIM profile (blue) with the 6 mJ experiment (red) and the 1.8 mJ experiment (yellow). Qualitatively compares nicely.

DEVELOPING THE CAPABILITY TO PERFORM MODERN STRESS CORROSION CRACK INITIATION TESTING ON PROTON-IRRADIATED MATERIAL

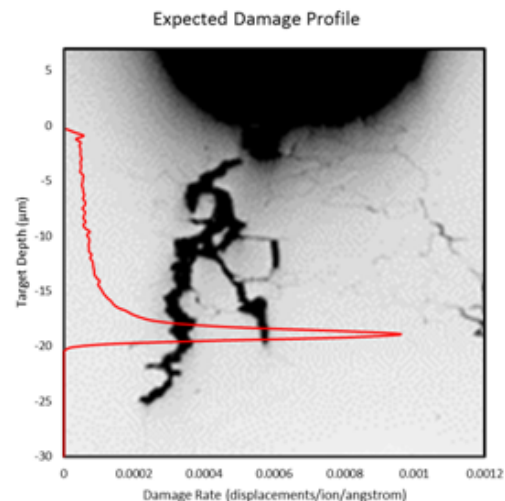
J.M. Smith, C.D. Judge, and S. Hanlon
Canadian Nuclear Laboratories (Chalk River Labs), Ontario, Canada

It is well known that the degradation of in-reactor materials by neutron irradiation can contribute to stress corrosion cracking (SCC) in instances where, in the absence of irradiation, cracking would not occur or would be considerably less severe. Irradiation-assisted stress corrosion cracking (IASCC) is a mechanism for which materials exposed to neutron irradiation become more susceptible to SCC with increasing fluence. While IASCC of austenitic stainless steels (SS) is a well-known active degradation mechanism in light water reactors, there are no known issues to-date for CANDU pressurized heavy water reactors. This is primarily due to the fact that, in the CANDU design, austenitic SS components are subjected to much lower neutron flux and temperatures (i.e., peripheral to the core). However, in the context of long-term operation, there is a desire to operate the current CANDU fleet for periods of up to 100 years. The combination of extended service life with the fact that irradiation-induced helium production likely precludes weld repair has heightened the concern regarding IASCC susceptibility.

Due to the considerable cost, time and complexity of radioactive material testing, there is a significant benefit to be realized by utilizing surrogate materials for the investigation of IASCC. This is especially true in the case of qualitative scoping tests for the rapid determination of relative susceptibility, sensitivity to key variables, or for the construction of databases. This methodology is extremely useful to narrow the overall investigation for comprehensive, neutron-irradiated studies, which can provide a check to a larger dataset. Simulating effects of neutron irradiation has been accomplished using ion irradiation techniques, which can be used to produce damage in the 1 to 5 dpa range in a day or two with very little residual radioactivity. While advantageous, a key drawback of ion irradiation for IASCC testing is that the damage is only produced in a thin “skin” on a sample surface. By leveraging CNLs expertise developed for in-situ detection of very short cracks (e.g., <math><10\ \mu\text{m}</math>), this project aims to develop a technique to use proton irradiation to simulate material damage at the base of blunt-notch, dog-bone tensile specimens fabricated from Grade 304 SS. Following irradiation, the direct current potential drop method will be used to monitor SCC initiation, under active tensile loading, in aqueous solution as a function of environmental variables. This technique is one of which intended for use in scoping tests to gauge the susceptibility of stainless steel components to IASCC in environments unique to CANDU reactors.



Crack length as a function of time.



Crack with superimposed damage profile.

IRRADIATION INDUCED DEFECTS IN METAL OXIDE ELECTRODE MATERIALS

K. Smith¹, J. P. Wharry², C. Xiong¹

¹Department of Materials Science & Engineering, Boise State University

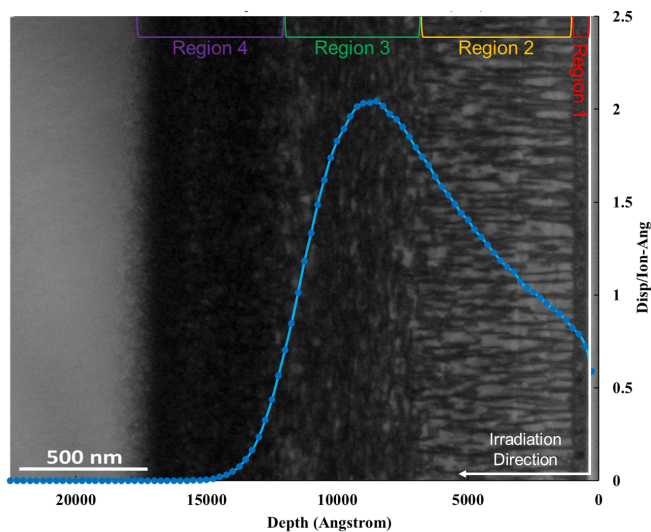
²School of Nuclear Engineering, Purdue University

Since their commercialization in 1991, lithium ion batteries have been the primary source of power in portable electronic devices. Future applications demand energy storage technologies that offer increased energy density and longer cycle life. Hence, recent studies have investigated enhanced electrochemical charge storage in electrodes that contain intentional structural defects. It is the goal of this project to investigate the fundamental effects of irradiation on TiO₂, and to understand how these effects can alter the electrochemical charge behavior when the oxide is used as an electrode in Li-ion batteries.

Rutile single crystal TiO₂ specimens were obtained from MTI Corp. for ion irradiation. The specimens are oriented such that the $\langle 100 \rangle$ direction is perpendicular to the ion beam. Irradiation with 3 MeV Nb⁺ ions was conducted in the 1.7 MV General Ionex Tandetron at the Michigan Ion Beam Laboratory. Cross-sectional TEM lamellae were milled by focused ion beam (FIB) in order to examine the range and accumulation of defects.

Four distinct defect regions were observed, ranging from the surface to a depth of ~1700 nm. These regions correspond to: (1) dense damage at the surface, (2) loops parallel to the irradiation direction along the positive slope on the SRIM damage profile, (3) loops perpendicular to the irradiation direction near the SRIM damage peak, and (4) damage corresponding to Nb implantation. While it is not unusual for irradiated rutile single crystals to exhibit different damage microstructures near the damage peak as compared to the near-surface region, none of the previous studies report a complex, multi-layered defect structure as that observed in this case. Furthermore, upon lithiation of the irradiated TiO₂ single crystal, preferential lithiation was observed within defects of the specimen, suggesting an affinity for lithium to diffuse into these damaged regions.

This work is supported by the National Science Foundation grant DMR-1408949.



SRIM calculation of defect distribution overlaid onto the TEM micrograph showing distinct defect regions in rutile single crystal TiO₂ resulting from Nb⁺ irradiation.

RADIATION-INDUCED SEGREGATION IN AUSTENITIC ALLOYS SUBJECTED TO PROTON IRRADIATION

M. Song¹, Chad Parish², M. Wang¹, G.S. Was¹

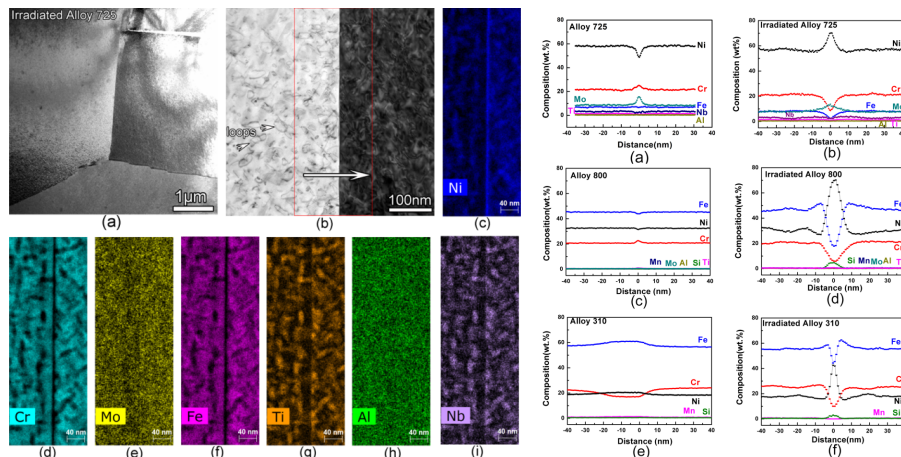
¹Nuclear Engineering and Radiological Sciences Department, University of Michigan

²Materials Science and Technology Division, Oak Ridge National Laboratory

Irradiation-assisted stress corrosion cracking (IASCC) is identified as one of the primary degradation mechanisms for materials of core components in light water reactors (LWRs) systems. Among all the factors, radiation-induced segregation (RIS), especially Cr depletion at grain boundaries (GBs), is suspected to be a contributor to the susceptibility of IASCC. The goal of this study is to evaluate the RIS behavior of nickel- and iron-based austenitic alloys 625, 625Plus, 625DA, 725, 800 and 310, which are rarely reported in literature.

All the alloys were proton-irradiated to 5 dpa at 360°C in the Michigan Ion Beam Laboratory (MIBL). Energy-dispersive X-ray spectroscopy (EDX) scans were performed on a Talos scanning transmission electron microscopy (STEM) in Low Activation Materials Design and Analysis Laboratory at ORNL. The selected random high angle grain boundary was tilted to an edge-on condition for EDX analysis. The EDX mappings were performed across the GBs (left figure). The 2D mapping data were transferred into 1D lines, corresponding to area with width of the box (>100nm) across the GBs (right figure). In nickel-base alloy 725, depletion of Ni, enrichment of Cr and Mo were observed in the as-received alloys. After irradiation, significant Ni enhancement was observed in the nickel base alloy while Cr and Fe were always depleted. Mo was a slow diffuser which is enriched in the as-received materials and depleted under irradiation. Segregation in as-received stainless steel 310 is insignificant, where only a small amount of segregation was observed. However, the RIS is significant. The general pattern is the same as in Ni-base alloys in which significant Ni diffuses to the GB and Cr and Fe diffuse away from the GB. The RIS of Si is pronounced, typically about 3 times its nominal value. In alloy 800, the amount of Si at the GB is comparable to that of Cr, while the nominal composition of Cr is more than 40 times that of Si in the alloy. These data constitute important knowledge of the RIS in commercial grade alloys.

This work is part of ARRM project that is supported by EPRI (contracts 10002164 and 10002154) and DOE (contract 4000136101). This work was also supported by the DOE NE under DOE Idaho Operations Office Contract DE-AC07-051D14517 as part of a Nuclear Science User Facilities experiment.



EDX mapping of irradiated alloy 725. (a) Bright field image of a triple junction (b) The target grain boundary and mapping area. EDX mapping results of individual element (c) Ni (d) Cr (e) Mo (f) Fe (g) Ti (h) Al and (i) Nb (left).

Grain boundary segregation before and after irradiation in several commercial grade alloys (a) as-received (AR) alloy 725 and (b) irradiated alloy 725(c)AR alloy 800 and (d) irradiated alloy 800 (e) AR alloy 310 and (f) irradiated alloy 310 (right).

EFFECTS OF PROTON IRRADIATION ON MICROSTRUCTURE AND STRESS CORROSION CRACKING IN ADDITIVELY MANUFACTURED 316L STAINLESS STEEL MADE BY LASER POWDER BED FUSION

M. Song¹, M. Wang¹, X. Lou², R.B. Rebak³, G.S. Was¹

¹Department of Nuclear Engineering and Radiological Sciences, University of Michigan

²Materials Engineering, Auburn University

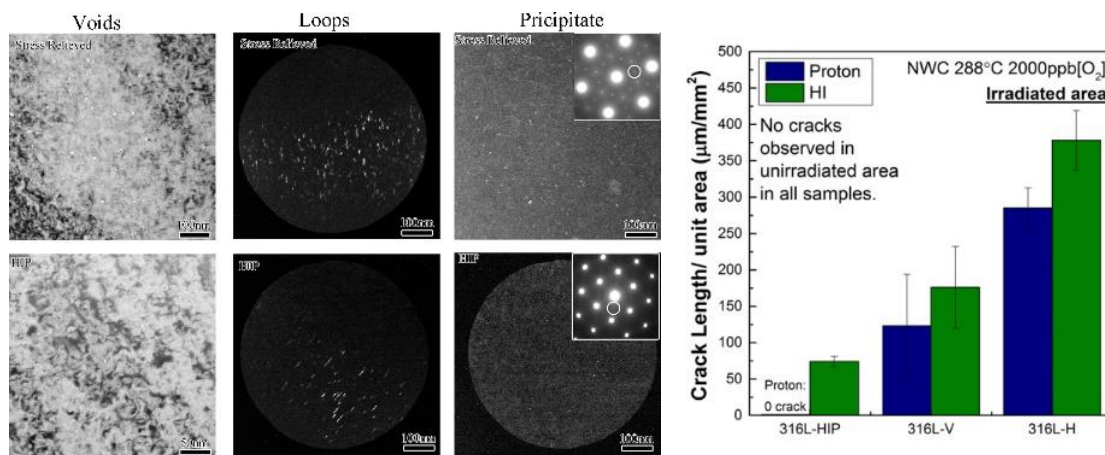
³GE Global Research, Niskayuna, NY

The nuclear industry has been exploring the use of 3D printing or additive manufacturing technology for reactor internals to enhance performance, shorten the supply chain, and reduce the cost and time to market. Additively-manufactured (AM) 316L stainless steel (SS) in the stress-relieved condition has demonstrated its potential for nuclear application. This study is a further evaluation of AM 316L SS by proton irradiation for microstructure stability and susceptibility to irradiation assisted stress corrosion cracking. The AM 316L alloys were proton-irradiated to 5 dpa at 360°C in the Michigan Ion Beam Laboratory (MIBL). Transmission electron microscopy (TEM) experiments were performed using a JEOL 3011 microscope operated at 300 kV. CERT tests were conducted at a strain rate of $1 \times 10^{-7} \text{ s}^{-1}$ in BWR 288°C simulated BWR normal water chemistry (NWC) environment to a fixed strain.

Significant microstructure changes were observed after irradiation in AM 316L SS. These microstructural features include voids, faulted dislocation loops, and γ' precipitate. Higher density of voids was observed in the stress-relieved condition ($2.4 \times 10^{21}/\text{m}^3$) compared with the hot isostatic pressing (HIP) condition ($5 \times 10^{19}/\text{m}^3$), despite the size are similar (8nm). Slightly larger loops (13nm vs. 8nm) were observed in the HIP condition compared with the stress-relieved condition but with a lower density (2.8 vs. $6.5 \times 10^{22}/\text{m}^3$). The density of the precipitates in the stress-relieved condition is an order of magnitude higher than that in the HIP condition ($5 \times 10^{21}/\text{m}^3$ vs. $3 \times 10^{20}/\text{m}^3$). No cracks were observed in the unirradiated conditions in all the conditions. Significant IASCC was observed. The HIP condition 316L had the lowest IASCC susceptibility while both stress-relieved conditions (vertically-built and horizontally-built) had higher susceptibility. The IASCC susceptibility is lower in proton irradiated samples than heavy ions one.

This study provides the first-hand knowledge of irradiated microstructure and irradiation-assisted stress corrosion cracking for AM 316L SS.

This work is supported by DOE (DE-NE0008428).



Irradiated microstructure of AM 316L SS in stress-relieved and HIP conditions (left). Cracking susceptibility of AM 316L SS in different conditions (right).

IRRADIATION-INDUCED NANOCLUSTER EVOLUTION IN Fe-9%CR ODS AND FERRITIC-MARTENSITIC ALLOYS

M.J. Swenson¹, J.P. Wharry²
¹Boise State University, ²Purdue University

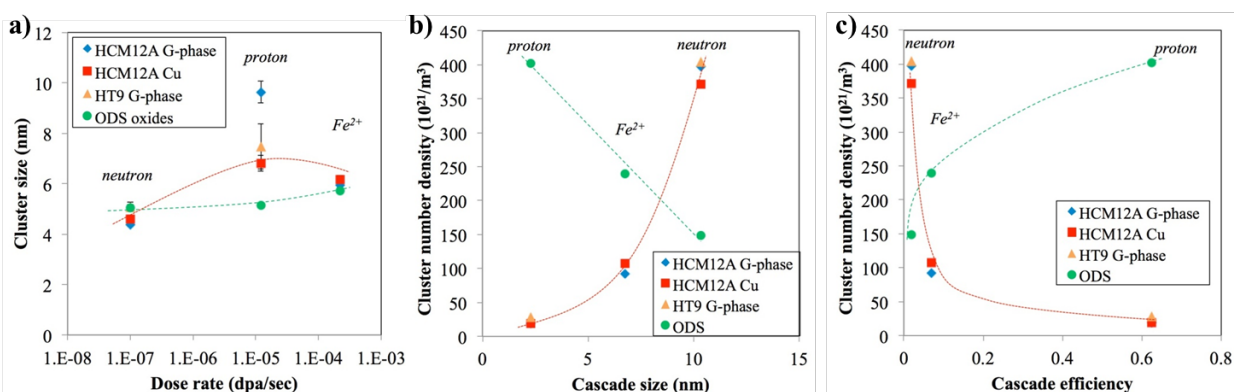
Charged particle and neutron irradiations have key differences that affect resultant microstructures: 1) dose rates typically differ by at least two orders of magnitude, and 2) irradiating particle types differ in damage cascade morphology. The consequences of these differences are unclear with respect to the mechanisms of solute nanocluster evolution. The objective of this study is to evaluate the effects of irradiation dose rate and damage cascade morphology on nanocluster evolution in a model Fe-9%Cr ODS steel and the ferritic-martensitic alloys HCM12A and HT9.

Specimens of each alloy were irradiated at MIBL to ~3 dpa at 500°C with either 5.0 MeV Fe⁺⁺ self-ions (~10⁻⁴ dpa/sec) or 2.0 MeV protons (~10⁻⁵ dpa/sec) and compared to earlier fast neutron irradiations at the same dose and temperature in the Advanced Test Reactor (~10⁻⁷ dpa/sec). The nanoclusters in each specimen are characterized using atom probe tomography (APT) and compared to their respective as-received samples.

As dose rate increases with particle type, the resulting size of nanoclusters in the ODS alloy tends to increase, which may be due to increasing coarsening rates resulting from higher rates of radiation-enhanced diffusion (RED). The same trend is less clear in the HCM12A and HT9 due to the proton-irradiated data, which may be due to an instable cluster size at such low dose. Regardless, the result of larger cluster sizes following higher dose rate irradiations is contradictory to the conventional positive temperature shift theory. To offset the effects of RED, a negative temperature shift may enable higher dose rate irradiations to emulate the solute cluster evolution of lower dose rate irradiations.

Meanwhile, both damage cascade size and efficiency are indicative of number density evolution of the nanoclusters. In the ODS alloy, number density declines with increasing cascade size, but increases with higher cascade efficiency. This trend suggests *inverse* Ostwald ripening is occurring due to the dominance of ballistic dissolution. Conversely, the opposite trends occur in the F/M alloys, suggesting Ostwald ripening occurs due to the preponderance of defect diffusion-driven growth.

This research was sponsored in part by the US Nuclear Regulatory Commission Grant NRC-HQ-84-14-G-0056 and by the US DOE, Office of Nuclear Energy under DOE Idaho Operations Office Contract DE-AC07-05ID14517, as part of the Nuclear Scientific User Facility experiments 13-419, 15-540, 15-569, 16-625, and 16-710.



Trends in ~3 dpa, 500°C nanocluster evolution: a) nanocluster size vs. dose rate, and nanocluster number density as a function of b) cascade size, c) cascade efficiency.

HIGH FIDELITY ION BEAM SIMULATION OF HIGH DOSE NEUTRON IRRADIATION

S. Taller¹, Z. Jiao¹, K. G. Field², G.S. Was¹

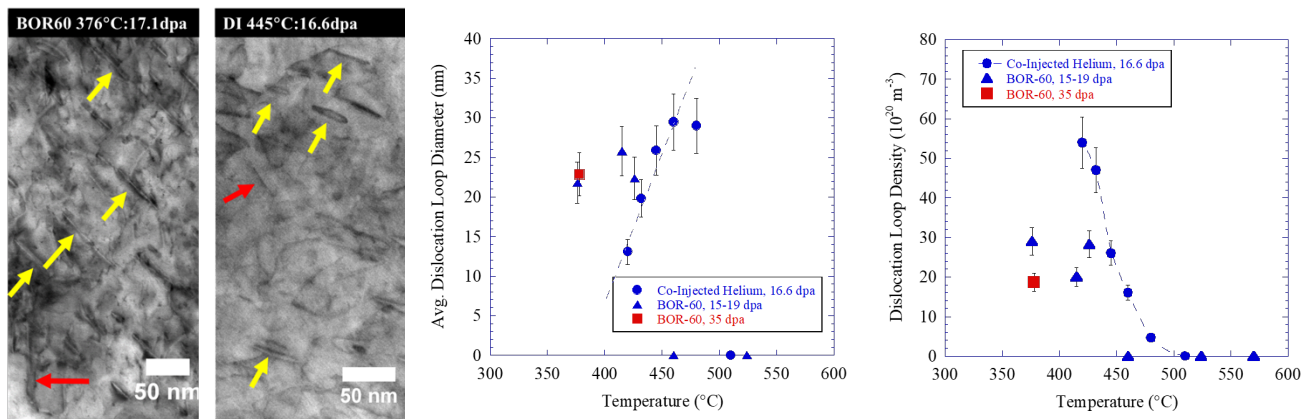
¹Department of Nuclear Engineering & Radiological Sciences, University of Michigan

²Materials Science and Technology Division, Oak Ridge National Laboratory

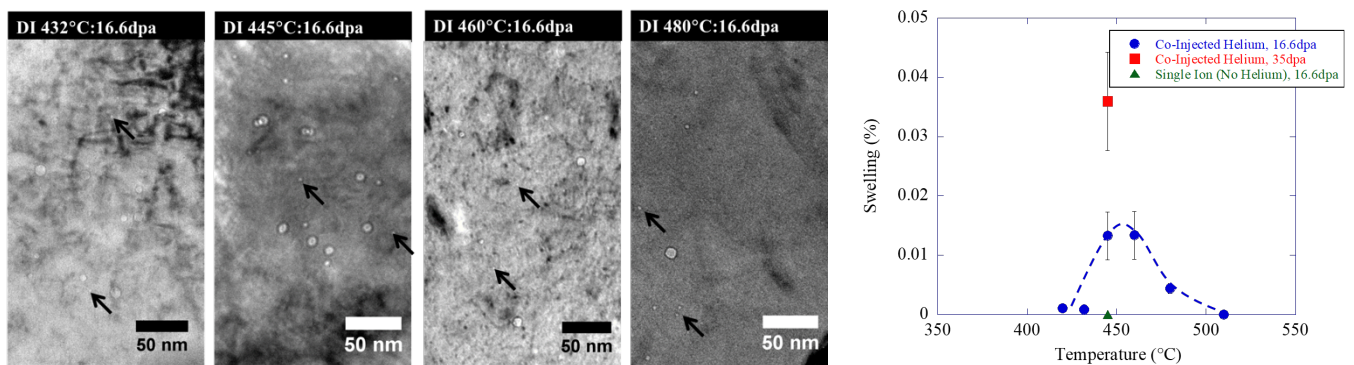
Traditional research efforts to understand radiation-induced processes in materials requires years of comprehensive post-irradiation characterization effort of test reactor produced neutron irradiated material. The same levels of radiation damage can be achieved using heavy ion irradiation under tightly controlled conditions in days or weeks instead of years in a nuclear reactor, albeit with several challenges. The purpose of this work is to address the use of ion irradiation experiments as a surrogate for neutron irradiation.

Several dual ion irradiations were performed using 5.0 MeV defocused Fe⁺⁺ ions to damage the material and simultaneously injecting He⁺⁺ ions in a fixed ratio to emulate gas buildup from nuclear transmutation reactions. Bars of T91 were dual ion irradiated up to 35 dpa with 0.22 appm helium per dpa from 420°C to 570°C to compare with multiple conditions from the BOR-60 fast reactor to the same level of damage and examine the role of temperature on the irradiated microstructure. These specimens are being examined with transmission electron microscopy and atom probe tomography to determine the effects of simultaneous helium injection and radiation damage on the irradiated microstructure of these materials.

This work is supported by the U.S. Department of Energy under award DE-NE0000639.



A comparison of STEM Bright Field (BF) images in T91 30176 irradiated with neutrons in BOR-60 or dual ions at MIBL (left) under [100] or [110] zone axis conditions to distinguish between a<100> (yellow arrows) and a/2<111> (red arrows) Burgers vector dislocation loops to determine dislocation loop density and average diameter.



Cavities were imaged in STEM BF and High Angle Annular Dark Field (HAADF). Cavities examined up to 1000 nm from the free surface of the ion-irradiated material in 100 nm increments. Underfocused TEM BF images are shown here for clarity of cavity observation with small bubbles highlighted with arrows. Cavities are visible as white spots with a darker fringe around it.

DEMONSTRATION OF THE CAPABILITY TO PERFORM MULTI-BEAM ION IRRADIATIONS AT THE MICHIGAN ION BEAM LABORATORY

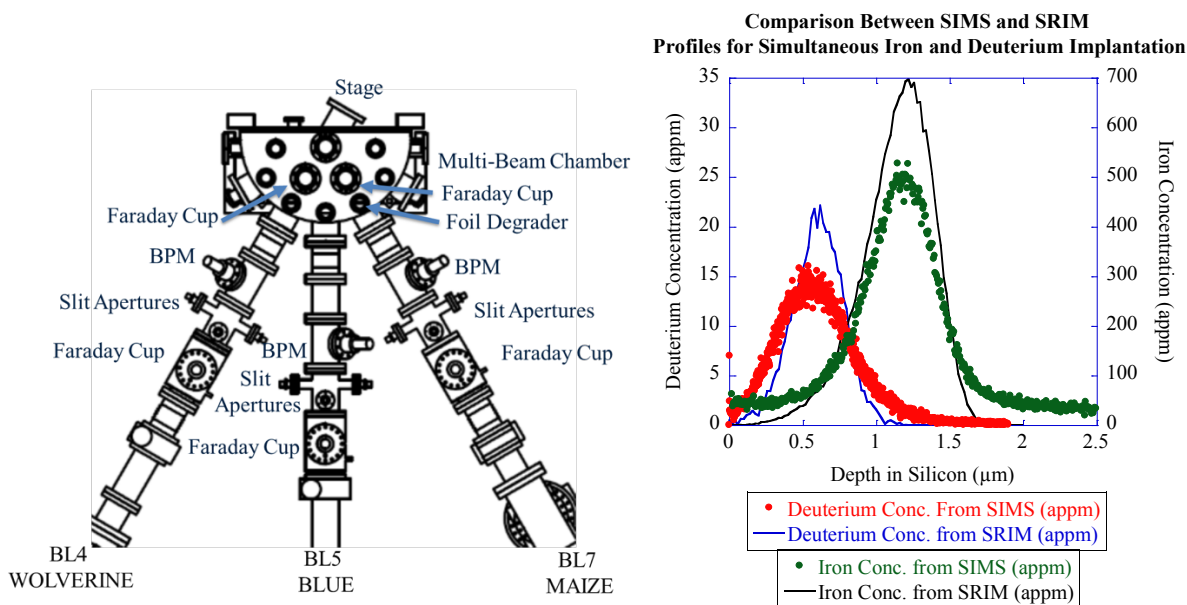
S. Taller, D. Woodley, S. Dwaraknath, Z. Jiao, G.S. Was
 Department of Nuclear Engineering & Radiological Sciences, University of Michigan

Material lifetime in nuclear reactors is limited by high levels of displacement damage to the microstructure, and by secondary or synergistic effects resulting from the buildup of gas from transmutation. Dual ion beam irradiation can be used as a surrogate for in-reactor irradiations to emulate this process with simultaneous irradiation of both a heavy ion beam and a light ion beam to induce damage and implant gas ions, respectively. This capability was developed at the Michigan Ion Beam Laboratory and a high fidelity demonstration of the efficacy of this technique is required before application to prospective reactor materials.

To demonstrate and benchmark the measurement systems for dual ion irradiations, a 1.34 MeV iron ion beam was defocused and implanted into a silicon wafer from the 3 MV Pelletron accelerator “Wolverine”. Simultaneously, a 940 keV deuterium beam from the 1.7 MV Ionex Tandem “Maize” was raster scanned over a 9.8 micron aluminum degrader foil designed for MIBL to reduce the energy and place the implantation peak of the deuterium closer to the surface compared to the implanted iron.

Concentration profiles with depth were measured using dynamic secondary ion mass spectroscopy (D-SIMS) and compared to profiles calculated using Stopping and Range of Ions in Matter (SRIM) for the same measured ion fluence during simultaneous implantation of iron and deuterium. The peaks of the calculated and measured profiles agree for both iron and deuterium, providing confidence in the energy loss calculations in SRIM. The measured peak concentrations are lower, but the integrated area under each profile agree strongly. This provides confidence in the measurement of the total amount of ions during multi-beam ion irradiations.

This work is supported by the U.S. Department of Energy under grant DE-NE0000639.



A top down drawing of the multi-beam chamber used for multi-beam irradiations at MIBL (left). SRIM predicted and SIMS measured concentration profiles with depth into silicon (right). The agreement of the integrated area under each profile provide confidence in the dosimetry of the experimental design.

RESOLUTION OF THE CARBON CONTAMINATION PROBLEM IN ION IRRADIATION EXPERIMENTS

G.S. Was¹, S. Taller¹, Z. Jiao¹, A.M. Monterrosa¹, D. Woodley¹, D. Jennings², T. Kubley¹, F. Naab¹, O. Toader¹, E. Uberseder¹

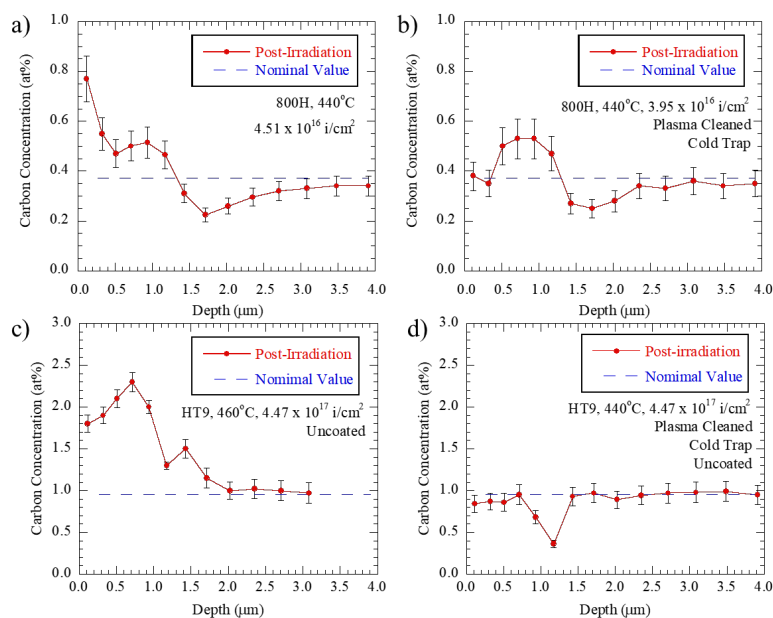
¹Department of Nuclear Engineering and Radiological Sciences, University of Michigan

²Materials Science Program, Colorado School of Mines

In the radiation damage community today, many laboratories are experiencing the pickup of carbon in their samples during ion irradiation. Carbon is incorporated into the irradiated microstructure, not just as a surface contaminant. The result is an alteration of the microstructure, most notably the formation of carbides, and modification of processes such as cavity evolution. Thus, it is carbon incorporation into the sample over the depth of penetration of the ion beam (0.1 to several μm) that is important. Most reports come from self-ion irradiation of iron and nickel-base alloys irradiated at high temperature. The widely experienced problem of carbon uptake in samples during ion irradiation was systematically investigated to identify the source of carbon and to develop mitigation techniques. Possible sources of carbon included carbon ions or neutrals incorporated into the ion beam, hydrocarbons in the vacuum system, and carbon species on the sample and fixture surfaces.

Secondary ion mass spectrometry, atom probe tomography, elastic backscattering spectrometry, and principally, nuclear reaction analysis, were used to profile carbon in a variety of substrates prior to and following irradiation with Fe^{2+} ions at temperature between 440-460°C. Ion irradiation of high purity Si and Ni, and alloy 800H coated with a thin film of alumina eliminated the ion beam as the source of carbon. Hydrocarbons in the vacuum and/or on the sample and fixtures was the source of the carbon that became incorporated into the samples during irradiation. Plasma cleaning of the sample and sample stage, and incorporation of a liquid nitrogen cold trap both individually and in combination, eliminated the uptake of carbon during heavy ion irradiation. While less convenient, coating the sample with a thin film of alumina was also effective in eliminating carbon incorporation.

This work is supported by the U.S. Department of Energy, Office of Nuclear Energy under the Nuclear Engineering University Program.



A comparison of the carbon concentration vs. depth profiles for alloy 800H (a and b) following irradiation to 20dpa with Fe^{2+} ions at 440°C and alloy HT9 (c and d) following irradiation to 188dpa with Fe^{2+} ions at 460°C without carbon contamination measures (left, a, c) and using plasma cleaning and a cold trap to prevent carbon incorporation (right, b, d)

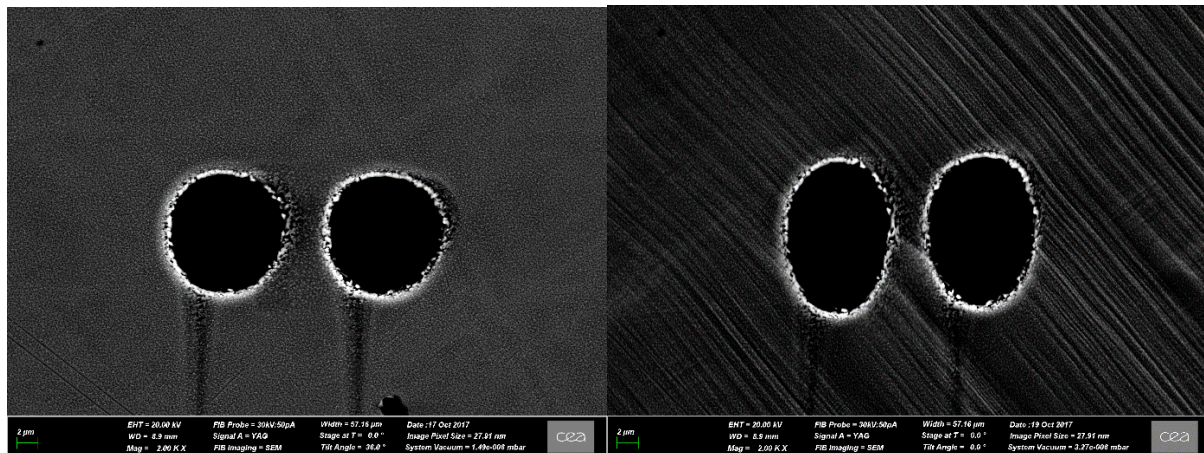
VOID GROWTH AND COALESCENCE IN 304L IRRADIATED STAINLESS STEEL.

P.O. Barrioz, J. Hure, B. Tanguy

CEA Saclay, Université Paris-Saclay, DEN, Service d'Etudes des Matériaux Irradiés, 91191 Gif-Sur-Yvette, France

304L Austenitic stainless steel used as structural materials in nuclear power plant are subjected to a flux of high energy neutrons. This lead to the creation of crystalline defects such as dislocations, dislocation loops, nano-voids and precipitates. The consequence is an evolution of the mechanical behaviors such as hardening, loss of strain hardening capability and loss of fracture toughness. In addition, mechanisms of deformation are modified, increase of strain localization with irradiation is observed. Analyze of dimples on the fracture surface of low to moderated irradiated stainless steel confirmed that the fracture mode of irradiated materials is still ductile. Therefore, study of void growth and coalescence is a key ingredient to better understand the loss of fracture toughness.

In order to enhance the ductile fracture models of irradiated stainless steel, it is important to know which mechanisms among hardening, loss of strain hardening and strain localization have to be taken in account. To answer that question, experiments are performed on 304L austenitic stainless steel irradiated with 2MeV protons to emulate neutron-irradiation. *Irradiation was performed at the Michigan Irradiation Beam Lab using a 2 MeV proton beam at 350°C with a fluence of $5.57 \times 10^{19} \text{ H}^+/\text{cm}^2$, which represents a calculated damage of 3.2 dpa.* This lead to a 20 μm irradiated layer on a bulk sample. Tensile samples containing only the irradiated layer are made by thinning down the bulk sample. Tensile samples fully irradiated in thickness are then obtain. Heat treatments were performed before irradiation to make the grains growth. It allows to drill intragranular cylindrical voids using Focused Ion Beam (FIB) in the tensile samples with a thickness of 20 micrometers. Growth and coalescence of the intragranular voids are observed as a function of plastic strain. High resolution Digital Image Correlation were performed in order to observe the strain localization. To do this, a speckle pattern are generated by the remodeling of a deposited gold layer. Speckle have a size around 100nm and a spacing around 150nm.



Initial and deformed void shape (12% plastic strain) in unirradiated sample. Loading direction is vertical.

ADVANCED AUSTENITICS (D9 ALLOY) FOR LWR APPLICATIONS

S. Teysseyre¹, M. Sokolov²

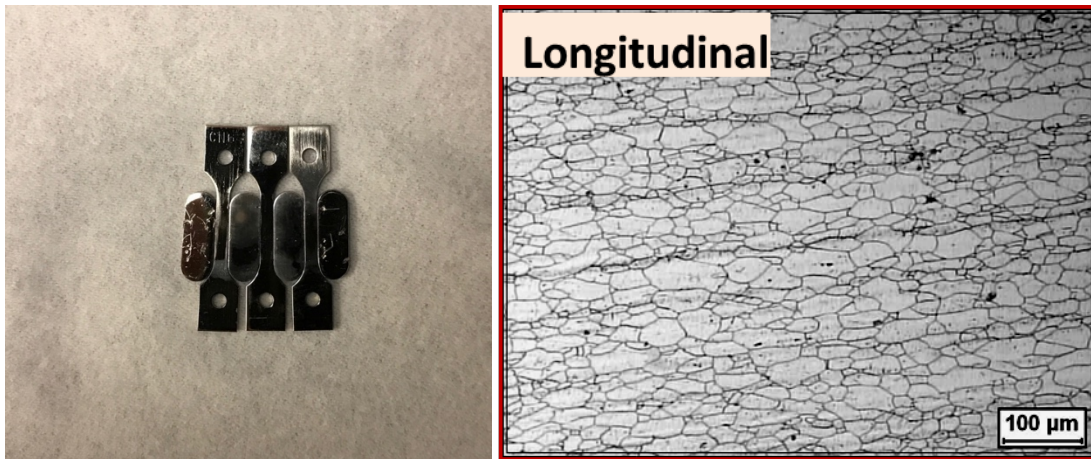
¹Idaho National Laboratory

²Oak Ridge National Laboratory

Ti-modified advanced austenitic stainless steel D9 (15Cr–15Ni–2Mo) has been identified as a potential candidate for use in nuclear core components of prototype fast breeder reactor (PFBR) program in India. Towards developing an improved version of alloy D9I for clad and wrapper of PFBR, a program investigated the properties of solution annealed and 20% cold worked D9 alloy with different compositions of minor alloying elements like Ti, Si and P.

The Indo-US civil nuclear energy working group is now investigating the potential of one of these advanced austenitic alloys for light water reactors applications. Solution annealed and 20% cold work materials have been characterized (metallography, chemical analysis, hardness, and tensile properties) prior to irradiation. A neutron irradiation campaign is underway in India to study the evolution of the material's properties as a function of accumulated fluence.

To study the influence of irradiation on the material microstructure and its susceptibility to stress corrosion cracking pre and post irradiation, slow strain rate tests (SSRT) will be performed in BWR and PWR water chemistries. In addition to neutron irradiation, protons irradiation will be used for this task. A set of 20% cold work specimens was irradiated to 3 dpa at a target temperature of 360°C using 2.0 MeV protons at the Michigan Ion Beam Laboratory (MIBL). The susceptibility of the three tensile specimens to stress corrosion cracking will be determined by SSRT in boiling water reactors' water chemistries. The data will be compared with the SSRT tests performed in our partner's facility with similar specimens that were neutron irradiated.



SS3 type specimens that were irradiated at MIBL(left).
Microstructure of the 20% cold work material in the longitudinal direction (right).

HEAVY ION IRRADIATION OF Fe-Cr MODEL ALLOYS

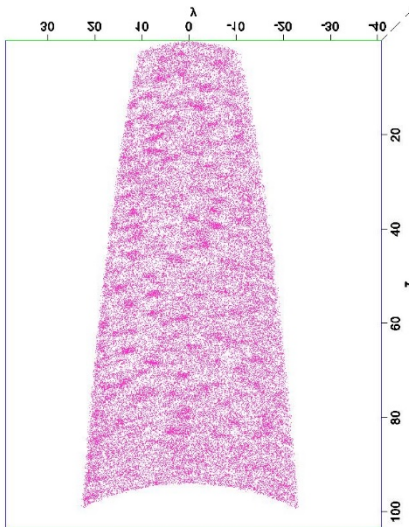
K.N. Thomas, Z. Jiao, G.S. Was

Department of Nuclear Engineering and Radiological Sciences, University of Michigan

High-chromium ferritic-martensitic (F-M) alloys are a candidate material type for future nuclear power plants due to the corrosion resistance and low swelling under irradiation. However, with chromium concentrations above $\sim 9\%$ and at lower temperatures below $\sim 500^\circ\text{C}$, the F-M alloys are susceptible to the formation of the Cr-rich α' precipitates. Research has shown that the α' precipitates can be formed under thermal aging, as well as neutron, electron, and proton irradiation, but there is difficulty in the α' precipitate formation under heavy ion irradiation.

In this study, model Fe-xCr ($x = 9, 12, 15, 18\text{wt}\%$) alloys were used. Ion irradiations were conducted at MIBL using 4.4 MeV Fe^{3+} at 300°C and at 400°C to 3 dpa with a dose rate $\sim 1.3 \times 10^{-5}$ dpa/s. The Cr-rich α' phase or precursors were observed in the Fe-xCr ($x = 12, 15, 18\text{wt}\%$) samples at 300°C to 3 dpa by atom probe tomography (APT), with continuing examination required for the remaining samples. This work also shows that it is possible to form Cr-rich α' phase or precursors through heavy-ion irradiation at low dose rates.

This work is supported by the U.S. Department of Energy under award DE-NE0000639.



APT reconstruction showing the formation of α' phase or precursors in Fe-18Cr irradiated to 3 dpa at 300°C .

IRRADIATION ASSISTED STRESS CORROSION CRACKING (IASCC) OF AUSTENITIC STAINLESS STEELS IN LIGHT WATER REACTORS (LWRS) ENVIRONMENT

M. Wang, M. Song, C. Lear, G.S. Was

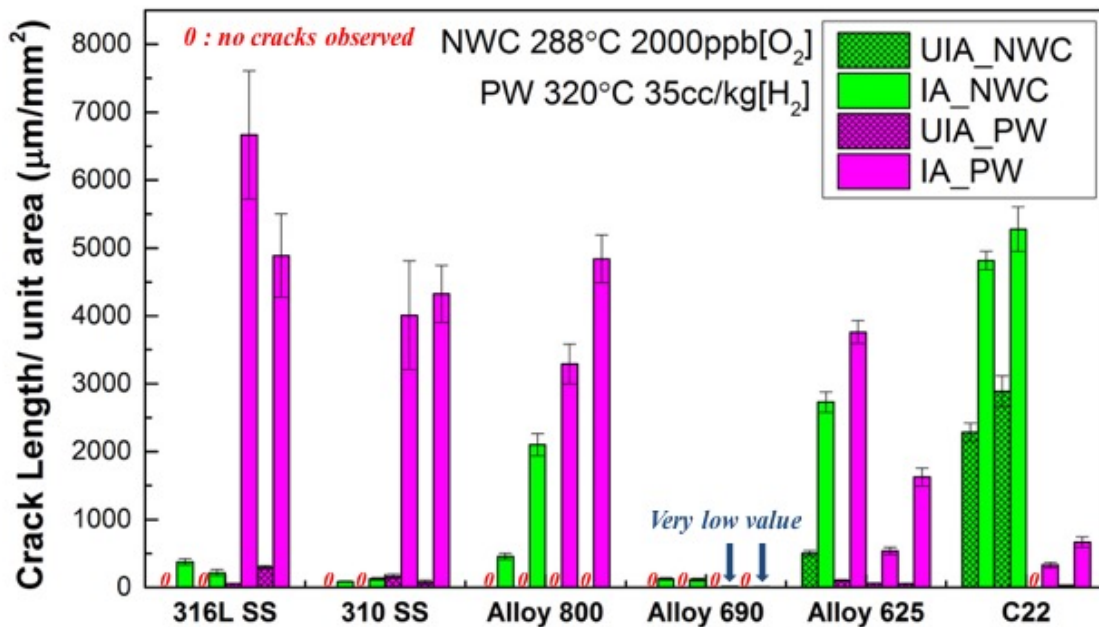
Department of Nuclear Engineering and Radiological Sciences, University of Michigan

The objective of Advanced Radiation Resistant Materials (ARRM) program is to identify the candidate alloys which have a high resistance of radiation induced damages, such as the irradiation assisted stress corrosion cracking (IASCC). This year, the IASCC behavior of low strength alloys, including stainless steels (316L, 310, alloy 800), nickel-base alloys (690, 625, C22) and advanced alloys (T92, 14YWT) were evaluated.

Samples were first irradiated by a 2 MeV proton beam to a dose of 5 dpa at a temperature of 360°C. CERT tests were conducted at a strain rate of $1 \times 10^{-7} \text{ s}^{-1}$ in both PWR (320°C PWR primary water with 1000 ppm B as H_3BO_3 , 2 ppm Li as LiOH, and 35 cc/kg H_2) and BWR (288°C simulated BWR normal water chemistry (NWC)) environments to a fixed strain.

Among all the low strength alloys, alloy 690 had the lowest IASCC susceptibility in both water environments while alloys 800 and 625 had relatively higher IASCC susceptibility. 316L and 310 both had much lower IASCC susceptibility in NWC than PW. However, C22 had lower IASCC susceptibility in PW due to its high Mo concentration. 14YWT and T92 were both necked at very early stage (around 2-3% plastic strain), thus no crack was observed.

The ARRM project is supported by EPRI (contracts 10002164 and 10002154) and DOE (contract 4000136101).



IASCC cracking susceptibility of different low strength alloys straining to 4% in both BWR-NWC and PWR primary water environments.

SHADOW CORROSION OF ZIRCALOY-2

P. Wang¹, G. S. Was¹, K. Nowotka²

¹Department of Nuclear Engineering and Radiological Sciences, University of Michigan

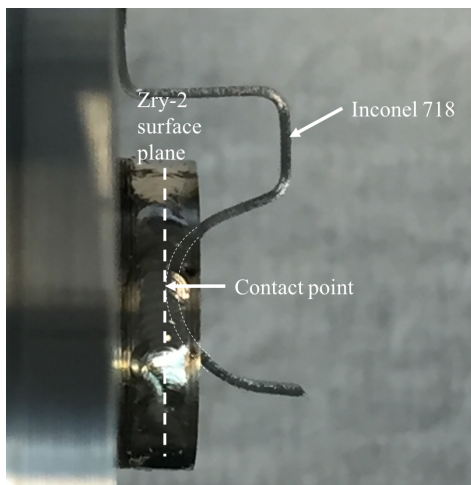
²Areva Germany

This project was aimed to continue with the 2016 project and optimize the experiments to maximize the shadow corrosion effect through modification of the sample design, by introducing a spring-loaded Inconel 718 that was in contact with Zry-2 sample surface shown in figure on the left.

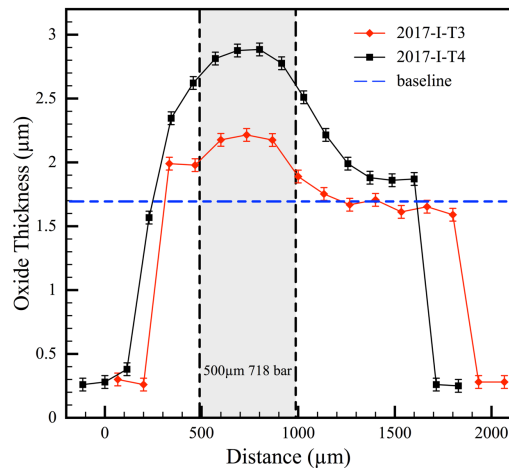
Several mechanisms have been proposed to explain the appearance of shadow corrosion, and the majority are related to the electrochemical nature of the Zircaloys. However, to date, shadow corrosion has only been observed on samples exposed in reactor. This implies the possible mechanisms by which radiation assists the shadow corrosion process; (1) by increasing the conductivity of the oxide film on Zr alloy, (2) by increasing the conductivity of the water by creating radiolysis products.

In this study, we have demonstrated that spring-loaded Inconel 718 produced a shadow more distinguishable than the previous designs. The shadow region can be clearly seen on the oxide thickness profile shown in the figure on the right. The contact region resulted in a large increase of corrosion rate, with an enhancement of 30-70% compared to the baseline values observed on a reference sample. Various coatings materials applied to the Inconel 718 spring has been tested and their effectiveness on shadow corrosion mitigation has been evaluated.

This research was supported by the AREVA Germany, Contract No.GF01/1016033557.



Side view of the new sample design with spring-loaded Inconel 718 in contact with the Zry-2 sample.



Oxide thickness profile perpendicular to the Inconel spring direction.

OXIDATION OF Fe-Cr-Al ALLOYS IN SIMULATED PWR ENVIRONMENTS DURING IN-SITU PROTON IRRADIATION

P. Wang¹, D. Bartels², G. S. Was¹

¹Department of Nuclear Engineering & Radiological Sciences, University of Michigan

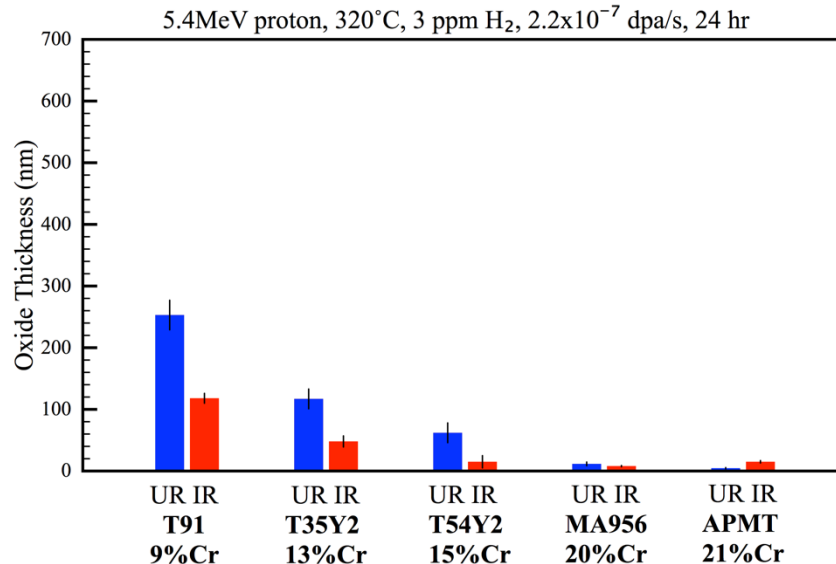
²Department of Chemistry and Biochemistry, University of Notre Dame

Following the high oxidation rate of fuel rods during the Fukushima Daiichi nuclear accident in 2011, the emphasis for nuclear fuel R&D activities has shifted to the development of accident-tolerance of LWR fuel. FeCrAl alloys were selected as one of the candidate materials for Accident-Tolerant Fuel application due to their excellent high temperature (1200°C) corrosion resistance in steam, greater strength, and they are very resistant to stress corrosion cracking. However, their general corrosion resistance is borderline and more importantly, no data exist on whether the iron-base alloys being considered for fuel cladding for ATF fuel are susceptible to irradiation-accelerated corrosion. There is also lack of understanding of the mechanisms by which corrosion rates are accelerated to be of any predictive value to the ATF program.

The objective of this work is to assess the corrosion behavior of ATF candidate iron-base alloys under normal LWR operating conditions consisting of high temperature, relevant water chemistry and irradiation.

In-situ irradiation-corrosion experiments have been performed on ATF candidate materials: T91, MA956, APMT, T54Y2 and T35Y2, in NWC and hydrogenated water chemistry using a 5.4 MeV protons beam. The resulting oxide thickness follows a trend that increases with decreasing alloy Cr concentration. APMT being the most corrosion resistance alloy. Inner oxide dissolution was observed on all alloys in the irradiated region, which radiolysis products and raised ECP was the main driving force for the dissolution of the inner oxide.

This research was supported by the DOE-NEUP, Contract No. DE-NE0008272.



Inner oxide thickness comparison of the ATF candidate alloys under and without the irradiation.

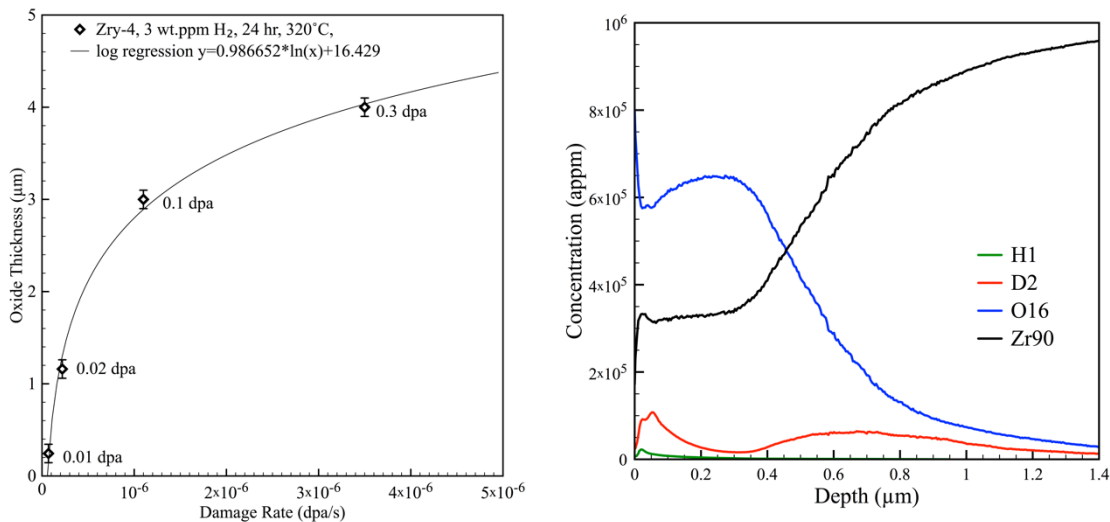
DOSE RATE EFFECT ON CORROSION AND HYDROGEN PICKUP FRACTION OF ZIRCOLOY-4 IN DEUTERATED PWR PRIMARY WATER USING IN-SITU PROTON IRRADIATION-CORROSION EXPERIMENTS

P. Wang, G. S. Was

Department of Nuclear Engineering & Radiological Sciences, University of Michigan

This project aims to understand how irradiation dose rate affects corrosion and hydrogen pickup behavior of zirconium alloy under PWR conditions. Multiple in-situ proton irradiation-corrosion experiments had been conducted to study the effect of damage rate on corrosion rate, and the resulting oxide microstructure was also analyzed. Corrosion rate of Zircaloy-4 follows damage rate logarithmically, and has a similar character as the parabolic/cubic corrosion kinetics under normal conditions. Microstructure of the oxide starts with columnar grain structure at low damage rate, and develops into a more equiaxed grain structure at high damage rate. Furthermore, oxygen diffusion coefficient was also determined for each damage rate and was compared to oxygen vacancy concentration with regards to the damage rate. A method to create standard sample of known concentration of deuterium in Zr for SIMS measurement was developed and tested. Hydrogen background and SIMS sensitivity of deuterium was comprehensively evaluated. A high-temperature heavy water exposed sample was also analyzed to determine its deuterium concentration and distribution, and it was determined that the hydrogen pickup fraction was consistent with literature values for pre-transition exposure.

This research was supported by the Consortium for Advanced Simulation of Light Water Reactors (CASL) under U.S. Department of Energy Contract No. DE-AC05-00OR22725.



Oxide thickness as a function of damage rate for multiple irradiation experiments conducted at 320°C for a duration of 24 h (left), and SIMS profile of the sample that was autoclave exposed in heavy water at 320°C (right).

IRRADIATION EFFECTS IN FERRITIC-MARTENSITIC STEELS AT VERY HIGH DAMAGE LEVELS

D. Woodley, Z. Jiao, K. Sun, G.S. Was

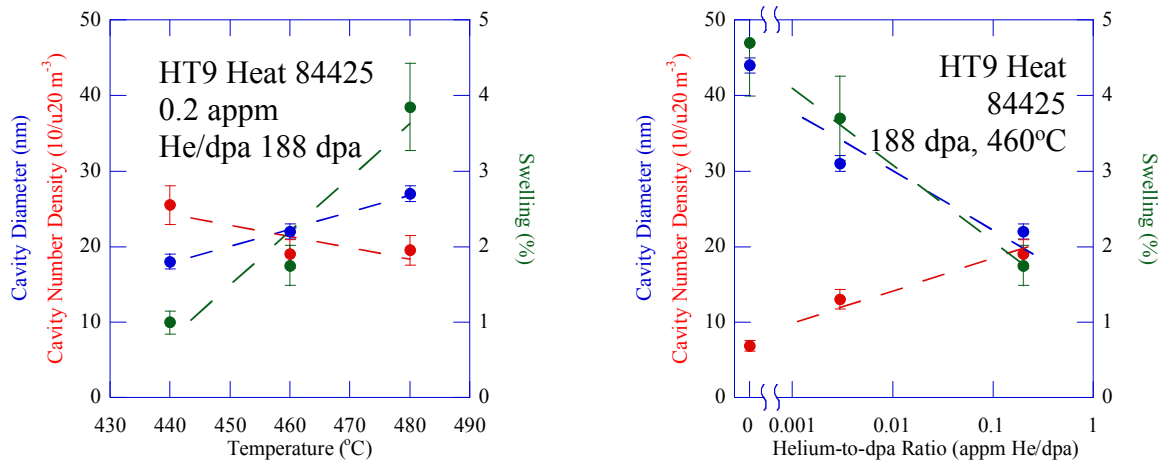
Department of Nuclear Engineering & Radiological Sciences, University of Michigan

Understanding the microstructural evolution in ferritic-martensitic steels is important for predicting the safety and reliability of future reactors. Dual ion irradiation experiments have been performed on heat 84425 of HT9, a ferritic-martensitic steel, to examine the effects of temperature and co-injected helium on dislocation loops, secondary phases and cavities. Irradiations were performed at the Michigan Ion Beam Laboratory with 5 MeV Fe^{++} ions from a 3 MV Pelletron accelerator and 2.05-2.18 MeV He^{++} ions, degraded through a rotating aluminum foil, from a 1.7 MeV Tandatron accelerator to simulate damage and transmutation gas, respectively. Experiments were performed to 188 dpa for temperatures from 440°C to 480°C at a constant helium-to-dpa ratio of 0.2 appm He/dpa and helium-to-dpa ratios of 0 to 0.2 appm He/dpa at a constant temperature of 460°C. The microstructural behavior was examined using both conventional transmission electron microscopy and scanning transmission electron microscopy. The dislocation microstructure, precipitate formation and cavity behavior were examined for each condition to map out the effect of temperature and helium on microstructural evolution.

Dislocation and precipitate evolution followed similar trends with temperature at a constant helium-to-dpa ratio. The loop and G-phase precursor diameters increased with increasing temperature while the densities decreased with increasing temperature. M_2X precipitates were not observed. Cavity formation was observed under almost all conditions. For a constant helium-to-dpa ratio of 0.2 appm He/dpa, cavity size increased with increasing temperature. Cavity density tended to decrease with decreasing temperature. The maximum swelling was observed at 480°C for a helium-to-dpa ratio of 0.2 appm He/dpa. In addition, bimodal cavity distributions were observed at all temperatures.

For a constant temperature of 460°C, dislocation loops and G-phase precursors were insensitive to changes in helium-to-dpa ratio. M_2X precipitates were not observed. In contrast, cavity evolution exhibited a strong dependence on helium-to-dpa ratio. A decreasing ratio led to a decreasing density and an increasing diameter. A bimodal cavity distribution was only observed at the highest helium level. The competing effects of lower cavity nucleation with higher cavity growth with a decreasing ratio led to a peak in swelling in the absence of helium.

This work is supported by the TerraPower, LLC.



Cavity diameter and density in HT9 heat 84425 as a function of (a) temperature at 188 dpa with a helium-to-dpa ratio of 0.2 appm He/dpa and (b) helium-to-dpa ratio at 188 dpa and 460°C. The plots ignore the bubbles and smaller cavities (diameter <10 nm) for the cases in which a bimodal distribution was observed.

TEM *IN SITU* CUBE-CORNER LAMELLA INDENTATION AND VIBE MOTION DETECTION ALGORITHM

K. H. Yano¹, J. P. Wharry²

¹School of Materials Engineering, Purdue University

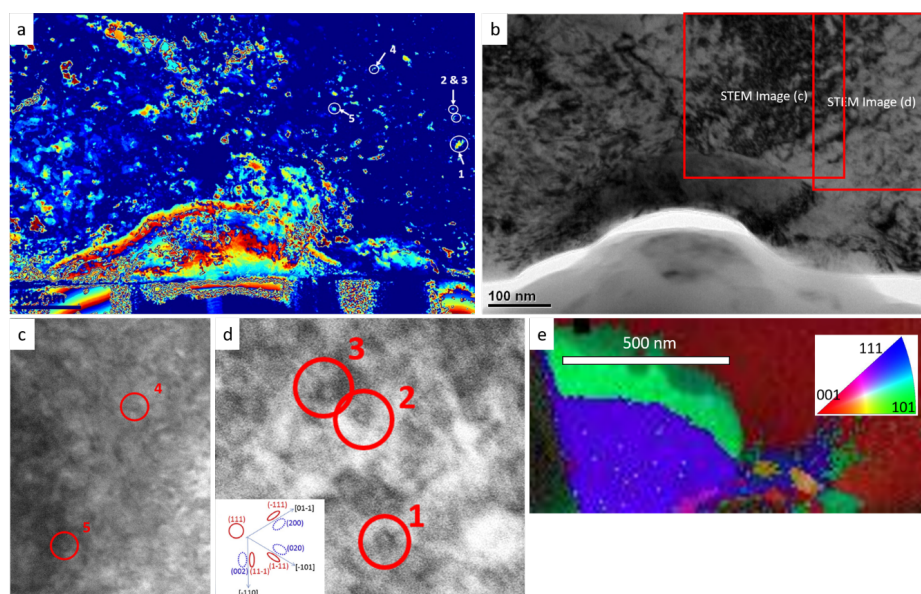
²School of Nuclear Engineering, Purdue University

Transmission electron microscopic (TEM) *in situ* mechanical testing is a promising method to understand the plasticity in shallow ion irradiated layers. One of the simplest such experiments is cube-corner indentation of a TEM lamella. However, the subsequent analysis and interpretation of the experimental results is challenging, especially in engineering materials with complex microstructures.

In this project, we conducted 5 MeV Fe²⁺ ion irradiation of a model Fe-9%Cr oxide dispersion strengthened (ODS) alloy at MIBL. We tested the irradiated ODS by cube-corner lamella indentation, recording the TEM video of the experiment. We then developed a motion detection and background subtraction-based post-processing approach, MicroViBe, and applied it to the recorded indentation video. Finally, we conducted post-mortem scanning TEM (STEM) imaging, to do an unbiased qualitative interpretation of the TEM indentation original and MicroViBe-treated videos.

MicroViBe identified changes in Laue contrast that were induced by the indentation. These changes then accumulated throughout the mechanical loading to generate a “heatmap” of features. Dislocation loops with $\mathbf{b}=\frac{1}{2} \langle 111 \rangle$ correspond to hotspots on the heatmap, whereas positions of dislocation loops with $\mathbf{b}=\langle 100 \rangle$ do not correspond to hotspots. MicroViBe offers a potentially new method for objective dislocation loop analysis and interpretation of TEM *in situ* indentation tests.

This work was supported by the US Nuclear Regulatory Commission Grant NRC-HQ-84-14-G-0056 and by the US DOE Office of Nuclear Energy under DOE Idaho Operations Office Contract DE-AC07-05ID14517, as part of the Nuclear Science User Facilities experiment 15-540.



Lamella indentation shown in (a) final heatmap, (b) final image after indentation with dislocation loops identified, (c-d) STEM images of respective areas identified in (b) showing dislocation loops, and (e) ASTAR image of entire lamella area above indentation

MICROSTRUCTURAL EVOLUTION IN NI-BASED ALLOYS UNDER IRRADIATION

L.-J. Yu, E. Marquis

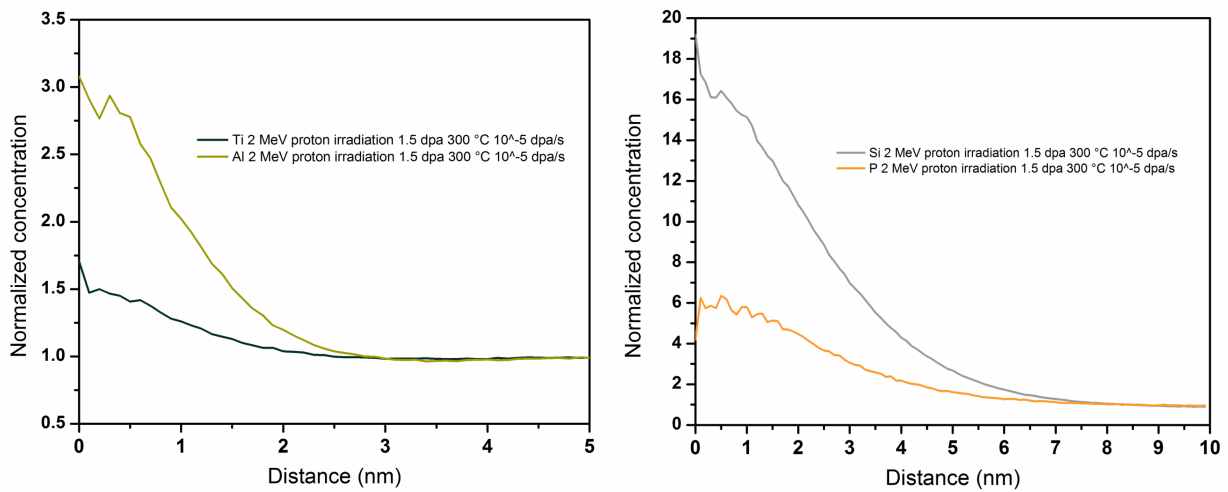
Department of Materials Science and Engineering, University of Michigan

As the operating lifetimes of nuclear power systems are being extended, the degradation of Ni-based alloys that have been used as structural materials in nuclear plants, under long-term thermal exposure and irradiation is a potential concern. For example, it has been reported that precipitation-hardened Alloy 625 softened during neutron irradiation due to precipitation dissolution. Ordered phases were also found in Alloy 625 after irradiation and in Alloy 690 after long-term thermal aging.

The objective of this research is to characterize the microstructural evolution of commercial Ni-based alloys under irradiation. Alloys 625, 625 plus, and 690 were irradiated to 1.5 and 6 dpa at 300 °C using 2 MeV proton at the dose rate of 10^{-5} dpa/s. The resulting microstructures were characterized using transmission electron microscopy and atom probe tomography.

Ordered regions in all three commercial alloys were revealed by atom probe tomography at the dose of 1.5 dpa. Radiation-induced segregation of impurities such as Si and P was detected and solute clustering such as Al and Ti formed after 1.5 dpa and the clusters became larger as dose increased to 6 dpa.

This work is funded by the Department of Energy Nuclear Energy University Program.



Radial distribution function of Al and Ti (left), and Si and P (right) showing clustering and segregation in Alloy 690 after proton irradiation at 1.5 dpa.

TEMPERATURE DEPENDENCE OF MICROSTRUCTURAL EVOLUTION OF Tm_2TiO_5 INDUCED BY HEAVY ION IRRADIATION

F. Zhang, L. M. Wang

Department of Nuclear Engineering and Radiological Sciences, University of Michigan

Irradiation effects of multiple cation oxides are of interest because they have been proposed as candidate materials in several nuclear energy related applications, including as nuclear waste forms, inert matrix fuel (IMF), and radio-frequency windows for fusion reactors.

Heavy-ion irradiation has been conducted on Tm_2TiO_5 to determine its radiation tolerance in a temperature range from 400°C to 700°C at a radiation dose of 20 displacements per atom (dpa). Irradiations were performed with 6 MeV Ag^{2+} ions using a raster beam with a 3 MV tandem ion accelerator at the Michigan Ion Beam Laboratory. The ion beam was aligned approximately normal to the sample surface. The temperature of the sample stage was controlled and monitored during irradiations.

Irradiation induced formation of dislocation loops and voids, as well as solid state amorphization have been observed in ion-irradiated Tm_2TiO_5 . A fully amorphized surface layer with thickness of ~500 nm was observed at 400°C. The thickness of the amorphous layer decreases with increasing irradiation temperature. A band of high density of dislocation loops developed in Tm_2TiO_5 below the amorphous band, and the depth of the dislocation loop band is also becoming shallower with the increasing temperature. The dislocation loop band is immediately in touch with the amorphous surface when the irradiation temperature was increased to 500°C or above. Voids were observed in the deeper depth of the irradiated samples. The distributions of amorphous layer, dislocation loops and voids are summarized in the Table.

Ion irradiation induced defects in Tm_2TiO_5

Temperature	Amorphous layer width	Amorphous layer depth	Dislocation band width	Dislocation band depth	Depth of voids
°C	nm	nm	nm	nm	nm
400	500	0 ~ 500	400	950 ~ 1350	2000
500	25	0 ~ 25	200	25 ~ 200	2100
600	20	0 ~ 20	150	20 ~ 150	1650
700	20	0 ~ 20	120	20 ~ 120	2000

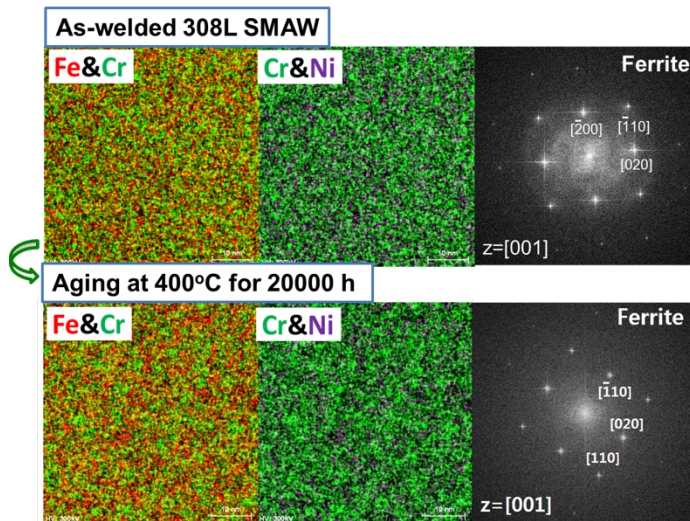
This work was supported by Shanghai Nuclear Energy Research and Design Institute (SNERDI).

EVALUATION OF THERMAL AGEING OF CAST AUSTENITIC STAINLESS STEEL (CASS) AND STAINLESS STEEL WELDS FOR LONG-TERM OPERATION OF LWRS

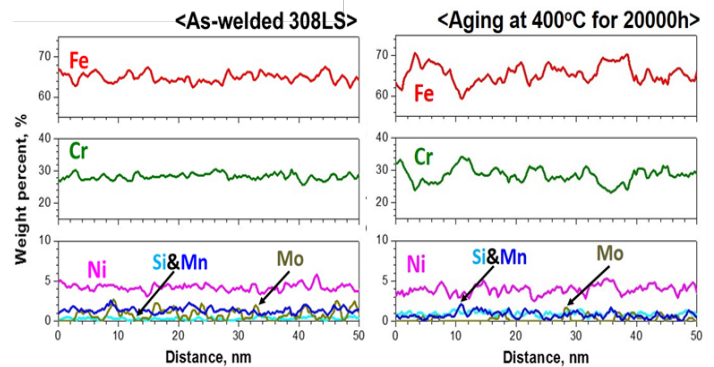
B. Song

Korea Advanced Institute of Science and Technology, Daejeon, South Korea

Cast duplex stainless steels (CASSs) and austenitic stainless steel welds (ASSW) are important materials in modern LWR facilities. Although currently operational LWR units have experienced very limited failures or material degradation concerns in the CASS and ASSW alloys during their design lives, thermal embrittlement (or zero ductility) above room temperature, however, has been observed in accelerated aging experiments. Currently, operation of the existing LWR power plants beyond their original design life is a key interest to the industry and government agencies. A significant knowledge base including experimental database obtained in realistic condition and thorough scientific understanding in aging degradation is needed to pursue operation beyond the typical design life of 40 years. In reality, however, there exists no operational experience for LWR beyond 40 years and no experimental data that can justifiably substitute for the operational experience. This research aims to fill major technological gaps regarding the aging degradation of massive stainless steel components, which will eventually enable the extended operations of LWR plants. This research aims to systematically build a scientific knowledge base for the thermal aging behavior of cast stainless steels (CASS) and their weld metals. The ultimate goal of this research is to reach a technical conclusion regarding the integrity of the CASS components of the current LWR fleet during the extended service life.



The results of TEM/EDS mapping result for as-welded and thermally aged 308L SMAW welds



The results of TEM/EDS line scan result for as-welded and thermally aged 308L SMAW welds

Teaching

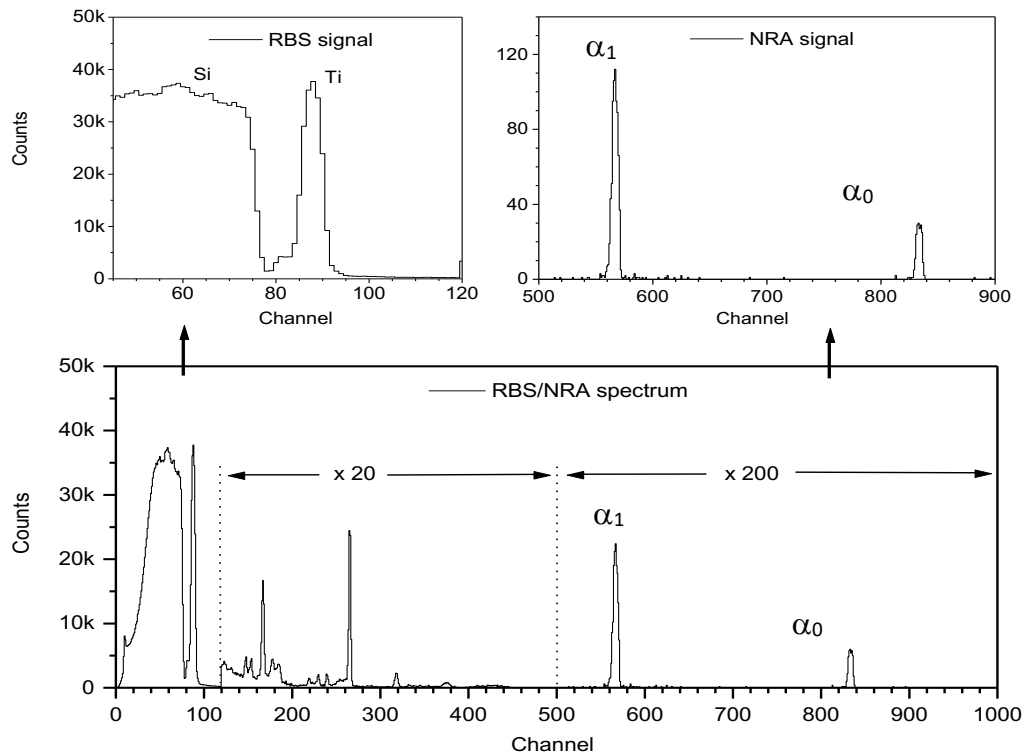
NERS 425 LABORTORY ON NUCLEAR REACTION ANALYSIS

G. Was, F. Naab, T. Kubley, E. Uberseder and O. Toader

Department of Nuclear Engineering and Radiological Sciences, University of Michigan

For one of the modules in the NERS 425 course, students conducted an experiment to determine the stoichiometry of a Ti_xN_y sample using the reaction between a deuterium particle and a nitrogen nucleus: $N^{14}(d,\alpha)C^{12}$. Nuclear reaction analysis (NRA) is a well-established surface analysis technique. In this method, an energetic particle, deuterium interacts with the nucleus of an N atom in the target to give a reaction product (α particle) that can be measured. The deuterium ion beam was produced by the SNICS ion source, using a TiD target, and was accelerated with the MAIZE Tandem accelerator. The students also use the backscattered yield from an RBS experiment to determine the amount of Ti in the sample by implementing simulation codes like RUMP or SIMNRA with the given experimental spectrum.

In the first meeting, prior to the experiment, a short tutorial was given to the students on the accelerator, electronics, detectors, software, and vacuum components. After that, they worked independently with just the basic support from the MIBL staff (required in the setup of the ion beam and the collection of the spectra). The students decided on a few parameters of the experiment (beam energy, time for spectrum acquisition, etc.), and obtained spectra similar to the ones in the figure.



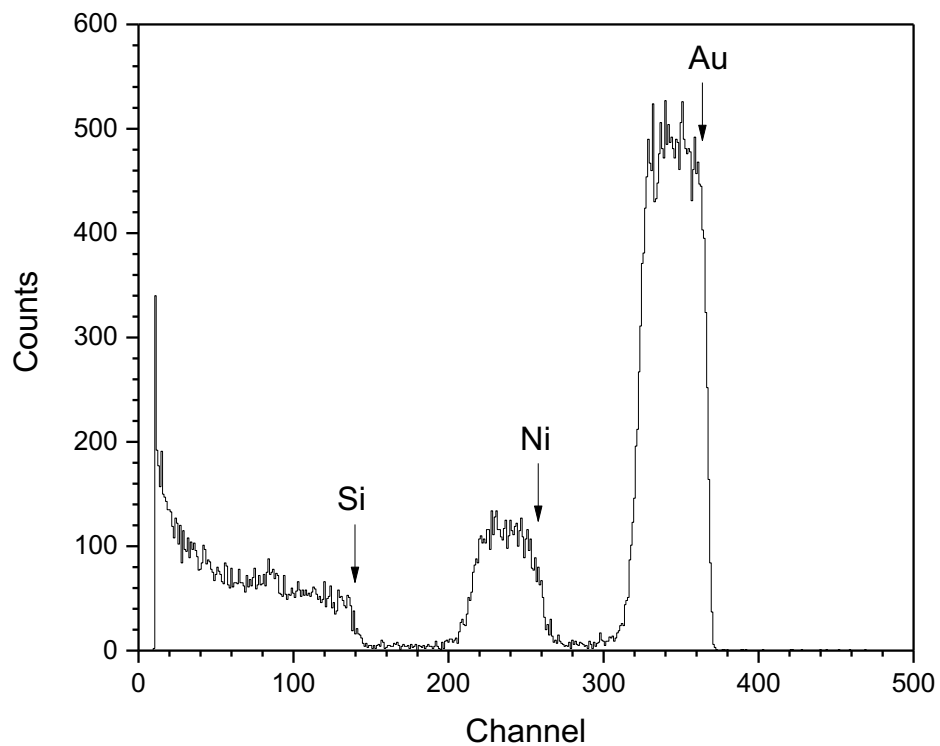
Typical RBS/NRA spectrum for the TiN film obtained during class.
Conditions: beam energy: 1.4 MeV D^+ , solid angle 5 msr., detector angle 150° .

MSE 465 CLASS DEMONSTRATION AT MIBL

S. Yalisove, E. Uberseder and O. Toader.

Department of Materials Science and Engineering, University of Michigan

MIBL hosted the MSE 465 class students (Structural and Chemical Characterization of Materials) for a session to tour the facility and to demonstrate Rutherford Backscattering Spectrometry, a topic covered in the class. A short tutorial was given on the accelerator, electronics, detectors, software, and vacuum components. After a few spectra were collected, some data was fit using SIMNRA software, a simulation package commonly used in these experiments. The spectrum collected for a gold and nickel film on a silicon substrate, is plotted below.



RBS spectrum of Au film and Ni film on a Si substrate. The spectrum was taken using a He^{++} ion beam at 2 MeV. The scattering angle was 160° .

PUBLICATIONS AND PRESENTATIONS

Publications

- W. Kuang, M. Song, P. Wang, G. S. Was, "The Oxidation of Alloy 690 in Simulated Pressurized Water Reactor Primary Water," Corr. Sci. 126 (2017) 227-237.
- L. Tan, B. Kim, G. Was, "Evolution Dependence of Vanadium Nitride Nanoprecipitates on Directionality of Ion Irradiation," J. Nucl. Mater. 495 (2017) 425-430.
- G. S. Was, S. Taller, Z. Jiao, A. M. Monterrosa, D. Woodley, D. Jennings, T. Kubley, F. Naab, O. Toader, E. Uberseder, "Resolution of the Carbon Contamination Problem in Ion Irradiation Experiments," Nucl. Instr. Meth. Phys. B 412 (2017) 58-65.
- S. Taller, D. Woodley, E. Getto, A. Monterrosa, Z. Jiao, O. Toader, F. Naab, T. Kubley, S. Dwaraknath, G. S. Was, "Multiple Ion Beam Irradiation for the Study of Radiation Damage in Materials," Nucl. Instr. Meth. Phys. B 412 (2017) 1-10.
- Mo-Rigen He, D. C. Johnson, G. S. Was, I. M. Robertson, "The Role of Grain Boundary Microchemistry in Irradiation-Assisted Stress Corrosion Cracking of a Fe-13Cr-15Ni Alloy," Acta Mater. 138 (2017) 61-71.
- S. A. Raiman, G. S. Was, "Accelerated Corrosion and Oxide Dissolution in 316L Stainless Steel Irradiated in-situ in High Temperature Water," J. Nucl. Mater. 493 (2017) 207-218.
- S. A. Raiman, G. S. Was, "Radiolysis Driven Changes to Oxide Stability During Irradiation-Corrosion of 316L Stainless Steel in High Temperature Water," J. Nucl. Mater. 493 (2017) 40-52.
- C. Silva, M. Song, K. Leonard, M. Wang, G. Was, J. Busby, "Characterization of alloy 718 subjected to different thermomechanical treatments," Mater. Sci. Engin. A 691 (2017) 195-302.
- C. D. Judge, V. Bhakhri, Z. Jiao, R. J. Klassen, G. Was, G. A. Botton, M. Griffiths, "The Effects of Proton Irradiation on the Microstructural and Mechanical Property Evolution of Inconel X-750 with High Concentrations of Helium," J. Nucl. Mater. 492 (2017) 213-226.
- T. Moss, G. Cao, G. S. Was, "Oxidation of Alloy 600 and Alloy 690: Experimentally Accelerated Study in Hydrogenated Supercritical Water," Metall. Trans. A 48A (2017) 1596-1612.
- T. Moss, G. S. Was, "Accelerated Stress Corrosion Crack Initiation of Alloys 600 and 690 in Hydrogenated Supercritical Water," Metall. Trans. A 48A (2017) 1613-1628.
- E. Getto, K. Sun, G. S. Was, "Characterization of M_2X formed during 5 MeV Fe^{2+} Irradiation," J. Nucl. Mater. 485 (2017) 154-158.
- E. Getto, G. Vancoevering, G. S. Was, "The Co-evolution of Microstructure Features in Self-Ion Irradiated HT9 at Very High Damage Levels," J. Nucl. Mater. 484 (2017) 193-208.
- S. Shaw, T. F. Silva, J. M. Bobbitt, F. Naab, C. L. Rodrigues, B. Yuan, J. J. Chang, X.C. Tian, E.A. Smith, L. Cademartiri, "Building Materials From Colloidal Nanocrystal Arrays: Molecular Control Of Solid/Solid Interfaces In Nanostructured Tetragonal ZrO_2 ," Chemistry of Materials, 29, 18, 7888-7900.

P. Mohapatra, S. Shaw, D. Mendivelso-Perez, J. M. Bobbitt, T. F. Silva, F. Naab, B. Yuan, X.C. Tian, E.A. Smith, L. Cademartiri, “Calcination Does Not Remove All Carbon From Colloidal Nanocrystal Assemblies,” Nature Communications, *accepted*

M.J. Swenson and J.P. Wharry, “Nanocluster irradiation evolution in Fe-9%Cr ODS and ferritic-martensitic alloys,” Journal of Nuclear Materials 496 (2017) 24-40.

K.A. Smith, A.I. Savva, C. Deng, J.P. Wharry, S. Hwang, D. Su, Y. Wang, J. Gong, T. Xu, D.P. Butt, and H. Xiong, “Effects of proton irradiation on TiO₂ nanotube electrode for lithium-ion batteries,” Journal of Materials Chemistry A 5 (2017) 11815-11824.

J.P. Wharry, M.J. Swenson, and K.H. Yano, “A review of the irradiation evolution of dispersed oxide nanoparticles in b.c.c. Fe-Cr alloys: current understanding and future directions,” Journal of Nuclear Materials 486 (2017) 11-20.

K.A. Smith, A. Savva, C. Deng, J.P. Wharry, S. Hwang, D. Su, Y. Wang, T. Xu, D.P. Butt, and H. Xiong, “Effects of irradiation induced defects on TiO₂ electrodes for lithium ion batteries,” The Electrochemical Society Meeting Abstracts, MA207-02.4 (2017) 419.

J.P. Wharry and K.H. Yano, “In situ TEM fracture testing for shallow ion irradiated layers,” Microscopy & Microanalysis, 23.S1 (2017) 738.

K.H. Yano, P.V. Patki, M.J. Swenson, and J.P. Wharry, “*Correlation between irradiation defects and transition dimension for TEM in situ mechanical testing*,” Transactions of the American Nuclear Society – 2017 Annual Meeting, 116 (2017) 22103.

P. Deng, Q.J. Peng, E.-H. Han, W. Ke, C. Sun, and Z. Jiao, “Effect of irradiation on corrosion of 304 nuclear grade stainless steel in simulated PWR primary water,” Corrosion Science, Vol. **127**, 91-100 (2017).

P. Deng, Q.J. Peng, E.-H. Han, W. Ke, C. Sun, H.H. Xia, and Z. Jiao, “Study of Irradiation Damage in Domestically Fabricated Nuclear Grade Stainless Steel,” Acta Metallurgica Sinica, Vol. **53** (12), 1588-1602 (2017) (in Chinese).

K. Ning, Z. Hu, K. Lu, “Spark Plasma Sintering of SiC-NFA Composites with Carbon Barrier Layer,” Journal of Nuclear Materials, 498, 50-59, 2018.

K. Ning, Z. Hu, K. Lu, “Spark Plasma Sintering of Silicon Carbide (SiC)-Nanostructured Ferritic Alloy (NFA) Composites with Chromium Carbide Barrier Layer,” Materials Science and Engineering A, 700 (17) 183–190, 2017.

Z. Hu, K. Ning, K. Lu, “Spark Plasma Sintered Silicon Carbide Ceramics with Nanostructured Ferritic Alloy as Sintering Aid,” Materials Science and Engineering A, 682, 586-592, 2017.

Z. Hu, K. Ning, K. Lu, “Study of Spark Plasma Sintered Nanostructured Ferritic Steel Alloy with Silicon Carbide Addition,” Materials Science and Engineering A, 670, 75–80, 2016.

K. Ning, Z. Hu, K. Lu, “Fabrication of New NFA-SiC Composites for Nuclear Applications,” 2016 American Nuclear Society Winter Meeting Proceeding, ISBN: 978-0- 89448-732-3.

Roger C. Walker II, Tan Shi, Bhakti Jariwala, Igor Jovanovic, Joshua A. Robinson, “Stability of the Tungsten Diselenide and Silicon Carbide Heterostructure against High Energy Proton Exposure”, Applied Physics Letters 111.14 (2017): 143104.

T. Shi, R. C. Walker II, I. Jovanovic, and J. A. Robinson, “Effects of Energetic Ion Irradiation on WSe₂/SiC Heterostructures”, Scientific Reports 7 (2017).

ER Reese, M Bachhav, P Wells, T Yamamoto, GR Odette, EA Marquis, “On α ’ composition in thermally annealed and neutron-irradiated Fe- 9-18Cr alloys,” Journal of Nuclear Materials (2017) 500, 192-198

ER Reese, N Almirall, T Yamamoto, S Tumey, GR Odette, EA Marquis, “Dose rate dependence of Cr precipitation in an ion-irradiated Fe-18Cr alloy,” Scripta Materialia 146 213–217 (2018) 146, 213-217

Presentations

“*Building Materials From Colloidal Nanoparticles*”, American Chemical Society Spring Meeting, Apr 2-6, 2017, San Francisco, CA

“*Plasma Processing of Colloidal Nanocrystal Arrays—A General Strategy for the Synthesis of Large Area Inorganic Mesoporous Materials*” Materials Research Society Meeting, November 26th-December 1st, 2017, Boston, MA

J.P. Wharry and M.J. Swenson. *Rate theory model for irradiation evolution of nanoclusters*. Materials Research Society Fall Meeting, Boston MA, November 2017. **INVITED**

K.A. Smith, A. Savva, C. Deng, J.P. Wharry, S. Hwang, D. Su, Y. Wang, T. Xu, D.P. Butt, and H. Xiong. *Effects of irradiation induced defects on TiO₂ electrodes for lithium ion batteries*. 232nd Electrochemical Society Meeting, National Harbor MD, October 2017.

J.P. Wharry and K.H. Yano. *In situ TEM fracture testing for shallow ion irradiated layers*. Microscopy & Microanalysis 2017 Meeting, St. Louis MO, August 2017. **INVITED**

K.H. Yano, P.V. Patki, M.J. Swenson, and J.P. Wharry. *Correlation between irradiation defects and transition dimension for TEM in situ mechanical testing*. American Nuclear Society 2017 Annual Meeting, San Francisco CA, June 2017.

H. Xiong, K. Smith, A. Savva, J.P. Wharry, and D.P. Butt. *Understanding irradiation effect on the structure and electrochemical charge storage properties of TiO₂ anode for lithium-ion batteries*. 12th Pacific Rim Conference on Ceramic and Glass Technology (PACRIM 12), Waikoloa HI, May 2017.

K.H. Yano, X.M. Bai, and J.P. Wharry. *In situ TEM cantilever testing of irradiated ODS to determine grain boundary embrittlement and cohesion*. The Minerals, Metals & Materials Society Annual Meeting, San Diego CA, March 2017.

Q.J. Peng, P. Deng, E.-H. Han, W. Ke, C. Sun, and Z. Jiao, “Effect of irradiation on corrosion of 304 nuclear grade stainless steel in simulated PWR primary water,” The 5th International Symposium on Materials and Reliability in Nuclear Power Plants, Shenyang, China, Sept. 26-28, 2017.

K. Lu, K. Ning, “SiC-NFA Composites for Nuclear Cladding Applications,” Frontiers in Materials Processing Applications, Research and Technology, Bordeaux, France, July 9-12, 2017.

K. Lu, K. Ning, K. Bawane, "Fabrication of Novel NFA-SiC Composites for Nuclear Applications," AFC Integration Meeting, Oak Ridge, TN, March 28-30, 2017.

K. Lu, "Material Needs and Developments in Energy Conversion, Harvesting, and Storage," Fifth Biennial Conference of the Combined Australian Materials Societies 2016, Melbourne, Australia, December 6-8, 2016 (Keynote).

K. Bawane, K. Lu, "High Temperature Oxidation of SPS Sintered NFA and Cr₃C₂-coated SiC-NFA Composites in Water Vapor Containing Environment," Materials Science & Technology 2017, Pittsburgh, PA, October 9-12, 2017.

K. Ning, K. Lu, "Corrosion Resistance of Pure SiC and SiC-NFA Composite under High Temperature Water Vapor Conditions," Materials Science & Technology 2017, Pittsburgh, PA, October 9-12, 2017.

K. Ning, K. Lu, "Study of SPS Sintered NFA and NFA-SiC Cladding Materials under High Dose Self-Ion Irradiation," Materials Science & Technology 2017, Pittsburgh, PA, October 9-12, 2017.

K. Ning, K. Lu, "Water Vapor Effects on SPS Sintered Nanostructural Ferritic Alloy and Silicon Carbide Composite Materials," Materials Research Society Fall Meeting, Boston, MA, November 27-December 2, 2016.

T. Shi, R. C. Walker II, I. Jovanovic, and J. A. Robinson, "Effects of Ion Irradiation on the Layered Semiconducting Material WSe₂", Poster Presentation, IEEE Nuclear and Space Radiation Effects Conference, July 2017.